A TECHNOECONOMIC ASSESSMENT OF ENERGY STORAGE POTENTIAL IN ARCTIC GRID SYSTEMS

Mallory Snowden

August 29th, 2025

Supervised by: Dr. Jacqueline Edge

A thesis presented to Imperial College London in partial fulfilment of the requirements for the degree of *Master of Science in Sustainable Energy Futures* and for the *Diploma of Imperial College*

Energy Futures Lab

Imperial College London

SW7 2AZ

Abstract

There are approximately 10 million people living in Arctic and Subarctic climates, 16% of whom rely on diesel-powered microgrids. The circumpolar region will be particularly difficult to decarbonise because of its harsh climate, paucity of trained workers, logistical barriers to new construction, and government subsidies tied to fossil fuel reserves. Moreover, Arctic outposts inherently prioritise energy security over decarbonisation, given the critical nature of heat and power outages.

Yet the conventional reliance on diesel generators is growing increasingly unsustainable due to volatile diesel prices, high transport costs, uncertainty about the future of fuel subsidies, and the impacts of climate change. Multiple Arctic communities have successfully adopted hybridised renewable energy storage systems to reduce their reliance on diesel. The deployment of energy storage is one of the most effective ways to increase the utilisation of variable renewable energy assets and displace diesel in remote Arctic grids.

The development of Arctic energy storage can often involve unforeseen costs and, in some cases, benefits. This study seeks to elucidate the effects of Arctic climate on levelised costs with the development of a deterministic, technoeconomic modelling tool. This tool builds upon a baseline cost model for energy storage systems in temperate climates to estimate the cost and performance changes associated with an Arctic counterpart. The competitiveness of lithium-ion, flywheel, pumped hydropower, compressed air, and hydrogen-based storage technologies was then mapped across a broad range of applications in the Arctic.

The levelised costs of pumped hydropower and compressed air storage were found to be most negatively impacted, mainly due to the heightened cost of large-scale construction in the Arctic. Hydrogen grid storage is less impacted and can even exhibit a reduction in levelised costs if the project allows for the exploitation of cold-temperature benefits such as improved energy density and reduced compression power. Lithium-ion-based storage systems are fairly resilient to Arctic climate, despite having a large performance decline below freezing. This is counteracted by their power-dense and modular architecture, which allows for efficient thermal management and minimal on-site construction costs. Flywheels are overall the least affected storage technology due to their modular, pre-fabricated architecture and their wide thermal operating range. The best storage option is highly project-dependent, and sensitivities of technology competitiveness to factors such as power level, power cost, discount rate, and maintenance costs are evaluated and summarised through the lens of Arctic storage development.

Table of Contents

List of Figures

List of Tables

List of Abbreviations

ACC - Annuitised Capacity Cost
A-CAES - Adiabatic Compressed Air Energy Storage
BESS - Battery Energy Storage System
CAES - Compressed Air Energy Storage
CF - Capacity Factor
CPY - Charges Per Year
CSP - Concentrated Solar Power
DD - Discharge Duration
DH - District Heating
DoD - Depth of Discharge
ESS - Energy Storage System
FEED - Front End Engineering Design
FESS - Flywheel Energy Storage System
LCOE - Levelised Cost of Energy
LCOS - Levelised Cost of Storage
LDS - Long Duration Storage
LFP - Lithium Iron Phosphate
NPV - Net Present Value
PCS - Power Conversion System
PEM - Proton Exchange Membrane
PGP - Power to Gas to Power
PHS - Pumped Hydroelectric Storage
PTES - Pumped Thermal Energy Storage
PV - Photovoltaic
ROI - Return on Investment
RTE - Roundtrip Efficiency
SEI – Solid Electrolyte Interphase
TES - Thermal Energy Storage
TMS - Thermal Management System
VRE - Variable Renewable Energy

1. Introduction

The circumpolar region is rich with renewable resources such as wind, summertime solar, geothermal, hydroelectric, wave energy, and biofuels [1], [2], [3], [4]. And yet many Arctic communities rely on imported diesel for heat and power despite its volatile prices, harmful environmental impacts, and unsustainable subsidies [3], [4]. The load profiles of Arctic grids show a high seasonal variation and a disproportionate demand for heating, which necessitates robust heat and power networks. Increasing the presence of renewable energy in the Arctic will reduce reliance on fossil fuels, but variable sources such as wind or solar require co-located storage to reach their full system benefit.

Stationary energy storage systems (ESS) have grown rapidly in recent years, with a record of 40% capacity addition (or 57 GW) in 2024 [5]. Assuming the global trends around electrification and variable renewable energy penetration continue, the need for grid-scale storage will increase exponentially [6]. Lithium-ion batteries are experiencing the highest growth rate of any storage technology with the greatest reduction in year-on-year price [6], [7]. However, lithium-ion batteries alone cannot meet global grid storage needs. This study aims to understand the climate and market conditions under which alternate storage technologies such as flywheels, pumped hydro, compressed air, thermal storage, and hydrogen become competitive from a technoeconomic perspective. Currently, storage modeling tools from publishers such as National Renewable Energy Laboratory (NREL) and Pacific Northwest National Laboratory (PNNL) either do not include climate effects or only cover a narrow range of storage technologies. The results from this study will help to inform storage developers of the key risks –and, in some cases, benefits– arising from building and maintaining ESS in the Arctic.

2. Key Factors Affecting the Future of Arctic Energy Systems

For the purposes of this study, “the Arctic” is defined as the regions with arctic and subarctic climates within the following eight countries: Canada, the US (Alaska), Russia, Norway, Sweden, Finland, Iceland, and Denmark (Greenland). Other regions such as Antarctica and parts of Mongolia and China exhibit low year-round temperatures; however, these areas are considered beyond the scope of this study.

2.1. Environmental Effects

Global warming disproportionately affects the Arctic, which exhibits surface warming rates of approximately four times the global average [8] . The resulting permafrost thaw and sea ice melt create a positive feedback loop which accelerates global warming via increased methane emissions and solar absorptivity [9]. Some arctic communities believe that global warming will benefit them on the whole, creating more arable land and milder winters [8]. However, this overlooks key considerations such as the endangerment of local wildlife, the disruption of indigenous hunting practices, the effect of sea level rise on Arctic ports, and the increased risk of extreme weather events such as flooding or wildfires [8]. As the pressure to decarbonise rises, government-sponsored diesel subsidies may decrease or disappear entirely [1]. This could incentivise an increased uptake of variable renewable energy (VRE) and ESS in Arctic communities. Despite global warming, the still-extreme temperatures of the Arctic must be considered with the deployment of new grid storage infrastructure.

2.2. Demographic Effects

The Arctic population is projected to be stable in the coming decades, with population growth in areas such as Alaska, Nunavut, Iceland, and Troms largely canceling out the population decline of Northern Russia [10]. Within the Arctic, there is increased migration from small communities to larger cities like Yakutsk, Russia or Reykjavik, Iceland [10]. The increase of urbanisation may signal a higher growth potential in large-scale energy storage projects over smaller microgrid installations.

2.3. Geopolitical Effects

Governments like Russia, the US, and China have shown increased interest in the Arctic for strategic military, shipping, and resource extraction purposes. Climate change has increased access to critical shipping routes such as the Northern Sea Route and Northwest Passage, which promise shorter trade paths between Asia, Europe, and North America [11], [12]. Additionally, as permafrost continues to thaw, previously inaccessible land becomes available for mineral extraction, including valuable resources like uranium and copper [11]. Sovereignty disputes over shipping routes and competition for larger shares of Arctic resources has increased the military and industry presence of Russia, which has recently commissioned or refurbished multiple airfields, military bases, deep-water ports, and border posts in the Arctic [12]. This may have been a contributing factor in U.S. President Trump's recent, though ultimately unsuccessful, attempt to purchase Greenland from Denmark [11]. The growth of military bases, heavy industry, and shipping ports in the Arctic (all of which rely heavily on fossil fuels) may present a setback to the deployment of renewables storage systems by improving the accessibility of oil & gas to surrounding communities. Alternately, this increased development may provide more opportunities for renewable energy and ESS integration as Arctic grid systems mature.

3. Current Energy Systems in Arctic Communities

Each Arctic territory employs its own favored technologies, subsidy scheme, and energy costs. More sparsely populated areas like Alaska, Northern Canada, and Russia rely heavily on fossil fuels [13]. Iceland, Norway, Finland, and Sweden are heavily grid-connected and use a large proportion of renewable power [13]. Table 1 shows the disparity in heat and power costs across the eight Arctic territories as well as the financial benefits of grid-connection. The high cost of transporting fuel to islanded grids incurs high prices and subsidies in diesel-dependent areas.

Country	Grid-Connected Cost of Power			Remote Cost of Power		Grid-Connected Cost of Heat			Remote Cost of Heat	
	Residential	Commercial	Industrial	Subsidized	Unsubsidized	Res.	Comm.	Ind.	Subs.	Unsub.
U.S. (AK)	13.0	10.7	6.9	24.3	46.2	3.5	2.6	2.0	11.5	
Russia	6.0	8.3	6.5	2.9–6.3	150.0	1.1		0.5		
Iceland	13.4	4.8	4.3							
Greenland	26.4			52.7		12.5			11.5	
Canada	11.0	8.8	8.9	17–42.0	114.0	2.6	2.7	1.0	15.2	18.9
Norway	32.5	5.0	10.0							
Sweden	22.0		8.9							
Finland	21.0	12.0	8.6							

Table 1: Average Cost of Power and Heat in Arctic Countries (2011-2020), in USD¢/kWh [13]

Alaska's most populated area, called "the Railbelt", stretches from the Kenai peninsula through Anchorage to Fairbanks. The Railbelt's interconnected grid system sources most of its power from natural gas, though it also uses coal, nuclear, and renewable generation [1]. The relative accessibility of the Railbelt, particularly in the Anchorage area, shields it from the high premiums paid in more remote areas, as shown in Table 1. It has been estimated that 140,000 people in remote Alaska comprise 13% of the state's energy demand, most of which is supplied by diesel fuel [1].

Canada's regional variation in power prices showcases how the integration of renewables can lower system costs. As of 2020, nearly three quarters of Canadian microgrids were solely dependent on diesel fuel [13]. The Yukon is Canada's only Arctic territory that uses predominantly hydroelectric power [13]. As a result, the Yukon's power prices are 77% lower than Nunavut and 64% lower than Northwest Territories including subsidies [3].

Greenland's power system is a regulated monopoly run by a state-owned entity called Nukissiorfiit [13]. The population of Greenland relies heavily on imported fossil fuels but also has significant hydropower capacity near the capital of Nuuk [13] [14]. Table 1 highlights the stark contrast between Greenland's grid-connected power prices, which are driven by local hydropower, and its remote prices, which rely on imported diesel.

Iceland, Norway, Sweden, and Finland are largely grid-connected with a small percentage of off-grid communities [13]. Iceland, which has a regulated monopoly power market and an almost entirely renewable power supply, enjoys cheap and stable utility rates [13]. This is largely due to the prevalence of geothermal district heating and hydroelectric power [13]. Norway, Sweden, Finland are deregulated power markets that trade through the Nord Pool exchange [13], [15]. These free markets experience more price volatility and less subsidisation than most Arctic regulated monopolies [15].

Russia, which accounts for more than half of the Arctic coastline, generally prioritises energy security over decarbonisation [8]. Arctic hubs like Murmansk and Yakutsk have GW-scale grids based largely on fossil fuels. In decentralised regions within the Far East and Arctic Zone, there are estimated to be 527 settlements with a cumulative population of over 300,000 [16]. The power generation in these regions is supplied mainly by diesel powerplants that sum to approximately 1 MW of capacity, half of which serves residential areas and half of which is allotted to mining outposts [16]. Many regions in Arctic Russia have aging infrastructure in need of upgrade and repair, but the state-affiliated utility companies can't finance major building projects without significant increases to local electricity tariffs [17], [18], [19]. Moreover, the grid infrastructure for many far-north communities is built upon melting permafrost [8].

4. Storage Technology Overview

4.1. Scope Definition

This study focuses on prevalent storage technologies from each of the following categories: electrochemical, mechanical, thermal, and chemical. Their suitability to the unique conditions and demands of Arctic communities will be discussed on a case-by-case basis. The strengths and weaknesses of each

storage technology are compiled in Table 2, along with their cold temperature effects and mitigation strategies. These will be discussed individually in Sections 8 through 12.

Technology	Pros	Cons	Cold-Temperature Adverse Effects	Cold-Temperature Mitigation Strategies	Cold-Temperature Benefits?
Lithium-Ion	•High RTE •Good Power + Energy Density •Fast Response •Modular, Pre-fabricated •Good economies of scale	•Hazardous + exotic materials •High marginal energy cost •Limited lifespan •Thermal runaway risk	•Charge/discharge rate reduction •Capacity loss •Power reduction •Accelerated aging	•Increased heating and insulation for BESS containers	•Reduced cooling power
Flywheel	•High RTE •Fast response •Long lifespan •Modular, Pre-fabricated	•Very high specific energy cost •High self-discharge rate •Low energy density	•RTE loss due to increased static friction	•Increased heating and insulation for modules and intermodal containers	•Reduced cooling power
PHS	•Low marginal energy cost •Good RTE •Long lifespan •Independent scaling of energy & power	•Slower response time •Large environmental impact potential •High CAPEX •Site-Specific	•Capacity loss due to ice formation on reservoirs •Power loss due to ice blockages upstream of the turbine	•De-icing mechansims, heaters, underground power station	•Negligible
CAES	•Provides LDS •Low marginal energy cost •Long lifespan •Independent scaling of energy & power	•Slower response time •Low energy density •Adiabatic CAES not fully commercialized •Site specific	•Lower enthalpy change across turbine at colder temperatures, resulting in lower RTE	•Increased air mass flowrate and compressor power	•Negligible
Hydrogen	•Provides LDS •Not site-specific •Partially compatible with existing O&G infrastructure •Independent scaling of energy & power	•Low RTE •High specific-power costs •Not fully commercialised	•Membrane Icing •Power reduction •Instability	•Increased heating and insulation for both PEM stacks and water tanks •Utilisation of exothermic heat for water system	•Improved energy density •Reduced compression power

Table 2: Comparison of key storage technology characteristics [6], [20], [21], [22], [23]

4.2. Electrochemical Storage

As mentioned previously, lithium-ion batteries are the fastest-growing stationary storage technology. Most new storage projects default to lithium-ion because of their low prices, high round-trip efficiency (RTE), and good combined power and energy density for low-to-mid discharge durations. An additional advantage of battery energy storage systems (BESS) in the Arctic is that they require minimal on-site assembly as compared with larger storage technologies like pumped hydroelectric storage (PHS).

On the other hand, lithium-ion BESS have high lifecycle emissions and rely on finite raw materials associated with negative environmental impacts, geopolitical dependencies, and unethical mining practices [7], [20], [24], [25]. As large-scale BESS installations increase, toxic battery fires have arisen in Queensland, Australia and Moss Landing, California— possibly increasing the insurance costs for similar projects [24], [26]. Lastly, lithium-ion batteries have a shorter operational lifespan and higher degradation rate than most other storage technologies [6], [7].

Low-temperature exposure has been shown to negatively affect the power output, energy capacity, (dis)charging rate, and ageing behavior of lithium-ion batteries. At cold temperatures, the battery's sluggish reaction kinetics and reduced ionic conductivity result in an increased internal resistance and a decreased power output [20], [27]. This slower ionic conduction means that during charging, lithium ions accumulate at the anode surface faster than they can intercalate into the graphite lattice [27]. This process is called lithium plating, and results in irreversible capacity loss. Another cold-temperature-driven failure mode involves damage to the solid electrolyte interphase (SEI) layer, which is a passivation layer that forms on the anode and protects it from undesirable reactions with the electrolyte. Exposure to extreme cold can cause excessive structural deformation of the anode which results in cracks on the SEI layer and direct contact between the anode and electrolyte, which in turn accelerates electrolytic decomposition [27].

A 2021 paper by Fly et al. presents performance data from the side-by-side testing of six different lithium-ion chemistries down to -40°C [20]. As seen in Figure 1, the performance of most cell types decreases dramatically below -20°C [20]. Ongoing research aims to improve lithium-ion cold-temperature performance through advanced cell materials and improved thermal management systems [20]. Sodium-ion batteries, though not fully commercialised, have been identified as a promising alternative to lithium-ion batteries in stationary storage applications, due in part to their improved capacity retention at low temperatures [28]. For stationary storage applications, sophisticated thermal management controls can ensure that batteries never exceed their thermal degradation threshold, at the cost of greater operational expenses.

Cell no.	Name	Technology	Positive electrode	Negative electrode	Nominal voltage/V	Rated capacity/mAh
1	Samsung 25R	Li-ion	$LiNiCoAlO_2$+$LiNiMnCoO_2$	Carbon+Si	3.6	2500
2	Sony VTC6	Li-ion	$LiNiCoAlO_2$	Carbon+Si	3.6	3000
3	Panasonic NCR18650b	Li-ion	$LiNiCoAlO_2$	Carbon	3.6	3200
4	Samsung 22P	Li-ion	$LiCoO_2$	Carbon	3.6	2150
5	GWL Power LTO18650	Li-ion	–	$Li_4Ti_5O_{12}$	2.4	1300
6	A123 APR18650m1A	Li-ion	$LiFePO_4$	Carbon	3.3	1100
7	GP410LAH	NiMH	NiOOH	Metal hydride	1.2	4100
8	Enersys RSACP3702	Lead-acid	Pb	PbO_2	2.0	2500
9	Green-Cap EDLC	Capacitor	Carbon	Carbon	2.7	500F

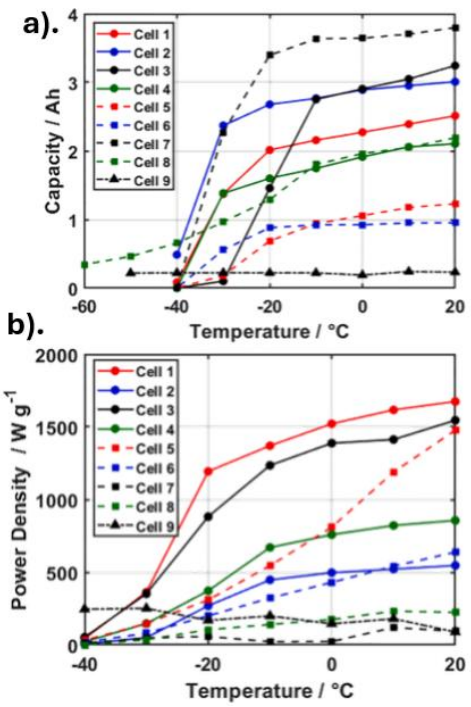

Figure 1: Cold temperature impacts on various battery chemistries: a). Discharge Test, b). Power Test [20]

4.3. Mechanical Storage

4.3.1. Flywheels

Flywheels charge and discharge using the acceleration and deacceleration of rotary inertia at extremely high speeds. Flywheels consist of a stator assembly and a rotor assembly. The stator assembly includes stationary components such as the control electronics, the motor-generator windings, the magnetic bearings, and the structural housing. The rotor assembly consists of a large, spinning mass with an array of permanent magnets which react with the electromagnetic field generated by the motor windings to convert AC power to kinetic energy and vice versa.

The application of flywheels is common in the transportation sector, where the kinetic energy of a vehicle's powertrain is partially recuperated via regenerative braking [6]. Flywheels have a high specific energy cost and self-discharge rate, and are thus best suited for fast-response, short-discharge power applications [6], [22]. They are most competitive in applications with high cycle frequency, where their superior lifespan results in lower replacement costs than an equivalent BESS. Flywheels show an excellent robustness to cold temperatures, but may require custom material choices and interface clearances for operation below -20°C [29].

4.3.2. Pumped Hydroelectric Storage

Pumped hydroelectric storage (PHS) charges by pumping water to a high elevation and discharges by using the water's gravitational potential energy as it flows downhill to drive a turbine. PHS has the most installed capacity to date but has limited future growth potential due to stringent site requirements [30]. Each PHS project is unique, with few opportunities to exploit economies of scale. Although PHS is currently the cheapest option for high-throughput, mid-to-long duration storage applications[6], its stagnant build costs and the price reduction of alternatives may result in future decline [6], [30].

Many regions of the Arctic have limited eligibility for PHS, and ice buildup in the reservoirs and tunnels can result in both energy and power capacity loss. However, PHS could be competitive in milder areas of the Arctic that require high-throughput storage— particularly in regions with existing dam infrastructure that could accommodate a PHS retrofit. Moreover, PHS has the unique ability to provide power storage while also preventing floods and regulating irrigation in the warmer months. This could become increasingly important as climate change causes accelerated glacial melt over the next 50 years [31].

4.3.3. Compressed Air Energy Storage

Compressed Air Energy Storage operates by using charging power to compress air into high-pressure underground caverns, which then discharges through a turbine to create power [6], [21]. CAES comes in two forms: Diabatic and Adiabatic. Diabatic CAES uses an external heat source to pre-heat the high-pressure air before it drives the turbo-generator. Adiabatic CAES stores the heat generated during the initial compression process to reuse later during the discharge process [6], [21]. Thus, Adiabatic CAES has a better RTE, lower emissions, and higher capital expense than Diabatic storage. Additionally, the proximity of waste heat sources can be used to augment the efficiency of A-CAES by charging the thermal storage further. However, A-CAES still has a lower RTE than pumped hydroelectric storage, and remains in the

early stages of commercialisation [6]. Another inherent limitation of CAES is its depth of discharge (DoD), since the storage pressure decreases as the system discharges. Some advanced plant concepts increase their effective DoD with the use of variable volume storage via flexible walls or hydraulic head, which helps to regulate the output pressure as the system discharges [32].

As of 2025, there are only three adiabatic CAES plants in operation – a small pilot plant in Canada and two large-scale plants in China. Additionally, there are three diabatic plants located in Germany, China, and the US, which makeup a collective capacity of approximately 700MW. There are no examples of CAES plants in the Arctic, though eligible sites for compressed air storage do exist [33]. The RTE of adiabatic CAES has been found to decrease slightly with ambient temperature, the cause and effects of which will be discussed in Section 11.1.

4.4. Thermal Storage

4.4.1. Thermal Energy Storage

Thermal energy can be stored in the form of sensible or latent heat. Sensible energy storage generally uses cheaper materials and has a wider range of acceptable storage conditions [34]. Latent energy storage uses phase change materials to increase the energy density, such as paraffin wax or salt hydrates. Latent energy storage is generally more expensive due to costly materials and encapsulation requirements [21],[34]. Heat can be stored in insulated tanks, underground caverns, or drilled boreholes depending on the project budget and land availability [34]. Thermal energy storage (TES) is an attractive option in regions with access to multiple sources and sinks, such as nearby waste heat from industry and district heating networks. In the Arctic, TES is a high-efficiency way to address periods of high heat demand. TES can also help to stabilise microgrids by storing excess power in the form of heat via electric boilers [1]. However, better insulation requirements could increase cost and decrease efficiency as compared to TES in milder climates. The tradeoff between insulation cost and efficiency loss should be considered when planning new TES projects [35].

4.4.2. Pumped Thermal Energy Storage

As thermal storage becomes more prevalent in Arctic regions, expanding the use cases beyond heating could be advantageous, particularly in communities without district heating networks. Increasing the options for both charging and discharging via multiple heat sources and end uses will improve system flexibility. Unlike TES, Pumped Thermal Energy Storage (PTES) can be used for both heat and power storage [23]. PTES involves pumping a working fluid (often air) through a circuit with two thermal storage tanks: one hot, one cold [23], [36]. During charging, PTES functions as a heat pump, with a compressor heating air to charge the hot storage tanks, followed by the air passing through a recuperator and expander to cool the cold storage tanks [23]. During discharge, the cycle runs in reverse— air is heated via the hot tank heat exchanger and expanded through a turbine to generate power via the Brayton cycle [23]. The greater the temperature difference between the hot and cold tanks, the higher the RTE, which generally ranges between 60-80% [23], [36], [37]. Unsurprisingly, the utilisation of waste heat from nearby industrial sources can significantly improve efficiency [37]. PTES could be a compelling alternative to CAES or

PHS due to its superior energy density, scalability, and thermal storage versatility— though adiabatic CAES will share the benefits of the latter. However, PTES is largely unproven at scale [23].

4.5. Chemical Storage

4.5.1. Hydrogen

Green hydrogen is the only form of chemical storage considered in this review. Green hydrogen is created from water and electricity through the application of a voltage beyond water's thermodynamic stability threshold which splits the molecule to form hydrogen gas. The hydrogen can then be stored and used to create power through a fuel cell or a gas turbine. Hydrogen as a means of electricity storage has the advantage of being site-agnostic, providing long discharge durations, independent energy and power scaling, and partial compatibility with existing oil and gas infrastructure. Key disadvantages include its low RTE and high capital expense [6], [38]. The high power input required to create green hydrogen necessitates proximity to low-cost power sources [2].

One application of green hydrogen is the back-to-back electrolyzer and fuel cell, which consumes power and water to discharge power and steam at up to 50% roundtrip efficiency [38], [39]. This Power-to-Gas-to-Power (PGP) technology is quite capital-intensive, though the experience curve in Figure 2 shows promising price improvements as fuel cell and electrolyzer installations grow [6].

Another option is to create hydrogen through an electrolyzer and combust it within a repurposed gas or diesel powerplant. Although preferable to fossil fuels, the combustion of hydrogen for electricity generation is less fuel efficient than a fuel cell and creates NOx, which is a potent greenhouse gas and an indirect air pollutant [39]. Additionally, the use of pure hydrogen would likely require upgrades to the plant's combustion chamber, fuel storage infrastructure, and safety systems [2]. However, a 2020 study from Dowling et al. estimates that the cost of building a new hydrogen combustion facility is approximately six times less than a comparable fuel cell system [38].

The most common electrolyzer and fuel cell technology is the Proton Exchange Membrane (PEM), which is vulnerable to icing at cold temperatures. Membrane ice formation causes instabilities, decreased power output, and possible damage to the electrolyzer or fuel cell [40]. Additionally, the electrolysis process requires large amounts of water on-site, which must be maintained in liquid form despite the Arctic climate. One advantage of Arctic PGP is that lower ambient temperatures can substantially improve its volumetric energy density, since the density of gaseous hydrogen increases with decreasing temperature. This has the secondary benefit of lowering compression power for systems that store hydrogen as a compressed gas.

5. Arctic ESS Case Studies

As previously stated, the deployment of storage alongside renewable generation increases the utilisation of renewable plants while reducing reliance on fossil fuels [1], [13]. Many case studies of real or modeled ESS were surveyed for this review, with common themes detailed below:

- Proper capacity sizing and integration of technologies is crucial for ESS viability [41] [42]

- Renewable energy coupled with ESS generally have higher upfront costs than standalone systems, and the payback period for Arctic ESS projects depend heavily on the integrated system design, reliability, cost of capital, and diesel prices [1], [2], [6], [41]
- Cost sharing on common infrastructure can reduce overall cost [1], [3], [38], [43]
- Less storage is required when the VRE mix (solar: wind capacity ratio) is optimised to match demand profiles [6], [44]
- Diesel is very hard to displace entirely in Arctic communities without other flexible generation sources such as hydropower [42]

The following sections will break down key findings of real or proposed ESS in the Arctic, as grouped by storage technology.

5.1. BESS in the Arctic

BESS generally pairs most efficiently with solar PV plants due to the diurnal cycle of charging and discharging, the modularity of both components, and a simpler DC-DC interface [41]. However, BESS can also be deployed as a backup power source or with wind energy to reduce curtailment, peak shave, avoid imbalance fees, and provide ancillary services such as frequency regulation [41]. In the far north, pairing a properly-sized BESS with bifacial solar PVs can enable the shutdown of diesel generators for most of the summer [4], [45].

A 2025 case study from Hosseini et al. assessed the financial impacts of replacing diesel with a Solar/Wind/BESS system. A genetic algorithm was used to optimise the relative capacities of wind, solar, and BESS within a given land space in Nunavut [42]. Four Nunavut communities with diesel microgrids were analysed, and historical power prices were compared to the hypothetical energy costs under a fully renewable scheme. It was found that the levelised cost of energy (LCOE) associated with eliminating the diesel backup entirely was too great, mainly due to the high number of batteries required. It should be noted that this study assumed the use of lead acid batteries at 220 USD/kWh and no long-duration storage (LDS). In the same study, an alternate proposal for a hybridised wind/solar/BESS/diesel solution theoretically improved power prices by up to 27% and reduced annual greenhouse gas emissions by over 55%, as compared with the diesel baseline [42].

The town of Kotzebue, Alaska realised early on that if their Power Cost Equalisation (PCE) subsidies were withdrawn, wind power would eventually become cheaper than diesel [1]. The PCE helps to moderate power costs in rural Alaska by subsidising utilities through the PCE Endowment Fund [1]. The first 50 kW wind turbines were installed in 1997, followed by larger wind turbines and eventually a zinc bromide flow battery in 2010 [1]. This BESS had many issues and ultimately didn't meet the system requirements, getting replaced by a 950 kWh Lithium Ion BESS in 2015 [1]. In 2021, bifacial PV arrays were installed amidst the wind turbines, sharing their inverter infrastructure and power cables to minimise cost [1]. Much of the upfront cost associated with this project was covered by state and federal grants, meaning Kotzebue enjoys reduced electricity prices and can lease its excess fuel storage to other local energy providers. Moreover, the battery system has greatly improved outages from both wind and diesel-related breakdowns [1].

In late 2022, Saft, a leading battery manufacturer, was contracted for a 6 MW/7 MWh BESS in Longyearbyen, Svalbard—the largest within the Arctic Circle. Designed to provide reserve power, black start capability, and grid stability, it supports the region's transition from coal. The installation is comprised of lithium iron phosphate (LFP) modules which are nominally rated down to -20℃, indicating that a customised solution has been created for this application [46], [47]. While there haven't been explicit updates on the plant in the news, it is presumably operational as of 2025 [47].

Meanwhile, a much larger LFP BESS facility was commissioned in 2023 for the Kenai peninsula in Alaska, reducing its natural gas consumption by 10%. This facility has an energy capacity of 93 MWh and utilises 37 Tesla Megapack containers. The project was commissioned three years after its first public announcement, with the CAPEX largely covered by a low interest loan from the U.S. Department of Agriculture [48].

5.2. Flywheels in the Arctic

Another interesting case is the island town of Kodiak, Alaska, which uses wind, BESS, and flywheels to balance rainfall-dependent hydroelectric power prices. The community of nearly 6,000 people utilises 9 MW of wind power with an integrated lithium-ion BESS and flywheel system [1]. The two 1 MW flywheels were installed in 2014 to support the integration of a 2 MW electric gantry crane in the shipping port [1], [49]. The regenerative power from lowering each shipping container charges the flywheels to power the crane's next lift. This technology enables the Kodiak Electric Association to handle large power spikes incurred by the crane in a small grid system (20 MW_{pk}). The two flywheel systems cost 4.02 million in 2025 USD, all of which was covered by a state Renewable Energy Fund grant [1], [49]. Assuming a lifespan of 25 years, this results in an Annuitised Capacity Cost of 80.40 USD/kW-year, which is competitive given the high number of annual cycles and the frequent replacements that would be required in an equivalent lithium-ion system [6].

5.3. PHS in the Arctic

Norway, which has the largest number of high-latitude PHS plants, uses them mainly for seasonal energy storage and flood management [50]. According to Pitorac et al.'s 2020 review of Norwegian pumped storage, PHS systems are typically open-loop, with a larger upper reservoir to enable flood management during the wet seasons of spring and fall [50]. This stored water is then released during the low-flow seasons to generate electricity when natural inflows are reduced. While Arctic PHS has traditionally been designed for infrequent discharges, this is changing as Norway diversifies its power mix with increased wind capacity, which requires higher frequency storage cycling. Some plants have been in operation for over 70 years, like Brattingfoss PHS which is located at 64ºN, illustrating the long lifespan potential even in harsher climates [50].

5.4. Thermal Storage in the Arctic

Thermal storage is significantly less expensive per kWh than electrical storage and has a superior operational lifespan [6], [34], [51]. Thus, in areas like the Arctic with nearly year-round heat demand, TES can be highly cost effective— particularly in regions with access to multiple heat sources and sinks [43].

Finland has numerous thermal energy storage projects in various stages of development. A company called Polar Night Energy has commissioned a 8MWh sand "battery" costing $200,000 in the city of Kankaanpää, Finland [52]. A large volume of sand is heated to 500-600°C via resistive heating elements and/or process heating from nearby industrial plants. The heat then discharges to supply district heating for the town's 12,500 inhabitants. Although the energy density of such a thermal battery is low, it is estimated to be eight times less expensive than a lithium-ion equivalent, and with a lower environmental footprint [52]. Additionally, the flexibility of charging from industrial waste and/or surplus grid electricity ensures low charging costs [52].

As renewable energy displaces diesel in many communities, it may be advantageous to repurpose some or all of the diesel infrastructure to support thermal storage. The Finnish city of Vaasa has demonstrated this in 2020, where the Vaskiluoto thermal storage system retrofits diesel tanks to store hot water as a thermal battery. Similar to Polar Night Energy's sand battery, this TES charges via waste-incineration and electric heaters during periods of wind excess [43]. Specific economic data on this project is limited, but the 11 GWh thermal battery reduces the city's coal consumption by 30% [43]. As of spring 2025, the developer, Vaasan Voima, is expanding the TES capacity to 17 GWh via upgraded electric boilers and an increased storage temperature [53]. This implies a high utilisation of their initial investment and a promising ROI for expansion.

While there are no operational or planned Arctic CAES plants as of 2025, thermal energy storage is an important component of adiabatic CAES, and many of its stabilisation and flexibility benefits apply for adiabatic CAES as well.

5.5. Hydrogen in the Arctic

While there are no operational hydrogen plants in the Arctic, there have been feasibility studies for pilot projects in Russia, Canada, and Iceland, among others [2], [8], [54], [55]. Green hydrogen is currently expensive and PGP is relatively unproven in extreme climates [6], [38], [40]. However, if PGP capital costs continue to drop, hydrogen could become economical in high-VRE grids [6], [38]. While multiple studies across the Arctic have shown that it is not economical to wholly replace diesel with green hydrogen at the current prices [2], [54], H_2 production has the potential to stimulate the local economy by attracting industries that use it as a feedstock while also supporting the grid.

The Moscow Institute of Physics and Technology has designed a novel hydrogen-based settlement in the Yamalo-Nenets region of Northern Russia [16]. This settlement, a remote research station called the "IAS Snowflake", aims to be the first hydrogen microgrid in the Arctic by the end of 2025 [56]. The settlement will use 300 kW of solar, 1.05 MW wind, 2.5 MWh BESS, and a 140 MWh electrolyzer to sustain 80 residents year-round [16]. The intent is for green hydrogen to be used as vehicle fuel as well as for power generation in conjunction with PEM-based fuel cells [16]. Limited information has been released on the build status or development cost of IAS snowflake as of August 2025.

6. Key Financial Metrics of Energy Storage

This section will describe the financial principles underlying ESS modeling, as any developer must understand the cost and revenue potential before undertaking a new storage project. The information below is a summary of relevant topics from *Monetizing Energy Storage* by Schmidt & Staffell through the lens of Arctic storage development.

6.1. Cost Breakdown

Storage costs are often given in power- or energy-specific format, depending on the type of storage services provided. The levelised cost of storage (LCOS) is used for applications that value energy, while the Annuitised Capacity Cost (ACC) is used for applications that value power [6]. The LCOS, typically shown in USD/kWh, is equal to the total lifetime costs divided by the total energy dispatched by a storage system. The ACC represents the total cost of providing a power capacity over a project's lifetime, shown in USD/kW-year. A detailed version of the LCOS calculation including discounting and degradation will be described in Section 7.

The main contributors to the levelised cost of storage are generally the investment cost, energy capacity, cycle frequency, and discount rate [6]. The discount rate, sometimes called the weighted average cost of capital, is generally correlated with project risk and determines how investors discount future cash flows to calculate the Net Present Value (NPV) of an ESS development. Projects with lower discount rate generally favor storage technologies with longer lifespans like pumped hydro, since future revenues are discounted less [6]. In the Arctic, there are multiple climate and accessibility factors that could incur higher discount rates and capital costs. This may bias private investors towards cheaper, shorter-lived technologies such as Lithium-Ion batteries.

As seen in Figure 2, storage costs generally decrease as capacity increases due to performance improvements and economies of scale. However, this does not necessarily hold true for mature technologies such as pumped hydropower storage [6]. Of the storage technologies included in Figure 2, lithium-ion and hydrogen have the steepest "experience curves", in terms of their price decline as a function of capacity expansion. The quantification of these trends in conjunction with market demand forecasts allows for the prediction of future storage costs.

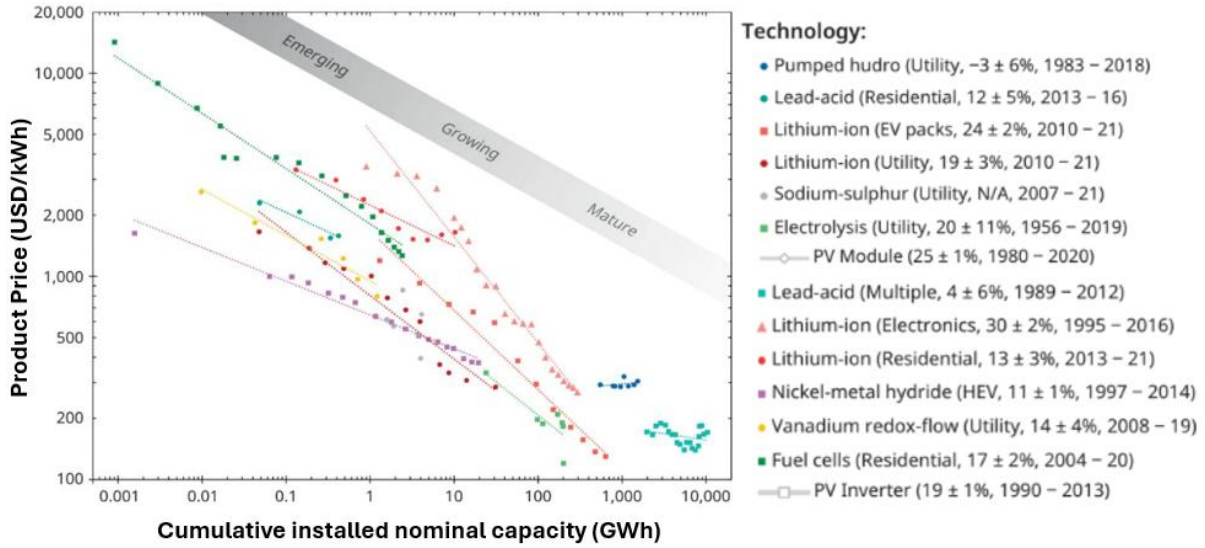

Figure 2: Global stationary storage price per kWh vs. installed capacity, normalised to 2020 USD [6]

6.2. Revenue Breakdown

The three main value sources of energy storage are as follows:

- Power Quality + Reliability
- Increased Asset Utilisation
- Arbitrage

Energy storage can help to keep grid systems within their voltage and frequency limits and bolster system resilience during deficits. Revenue from the provision of power quality or reliability typically comes from grid operators through mechanisms such as frequency response auctions or capacity markets. In many Arctic power markets that follow a cost-of-service model, the value of providing quality and reliability can be quantified as the system cost savings of avoiding outages.

Storage can also increase the utilisation of variable renewable energy (VRE) assets that would otherwise face curtailment during periods of excess. The value of storage to enable increased asset utilisation can be quantified through the savings of 1). purchasing less fuel via increased VRE output, and 2). avoiding costly construction projects.

Arbitrage is the practice of charging a storage system during off-peak hours and then discharging at higher, on-peak prices. Arbitrage is not considered as a potential revenue stream for areas with regulated power prices and would only be relevant for ESS in deregulated markets such as Norway, Sweden, or Finland.

In reality, the profitability of ESS is tenuous, and storage systems will generally need to provide multiple grid services to be financially viable [6]. In deregulated power markets, energy storage can compete for contracts to provide grid services or participate in arbitrage. In smaller regulated monopolies such as Greenland or Nunavut, storage revenues are reframed as long-term cost savings [1].

This study will focus on modeling costs rather than revenues as revenues are considered constant for a given application, regardless of the storage technology— provided that the technology can meet the required response time, power level, and discharge duration. Thus, the key financial differentiator between storage options for a new project is the LCOS or ACC.

6.3. Financial Modeling of Storage Systems

Multiple industry tools such as HOMER and ReOpt can estimate a project's LCOS with user-defined inputs such as power level, power cost, and discharge duration [57] [58]. However, none of these tools have the ability to compare the technoeconomic performances of multiple storage technologies while incorporating their climate-specific characteristics.

Figure 3, which was generated by the tool StorageNinja in 2023, shows a visualisation of the competitive storage landscape for a range of applications and storage technologies [6], [59]. This log-log plot is generated using probabilistic uncertainties assigned to key parameters such as capital cost, RTE, and cycle life for each storage technology before assessing their relative cost competitiveness across a wide range of applications [6]. A key question of this study is how this competitive ESS landscape would shift when Arctic-specific factors are taken into consideration.

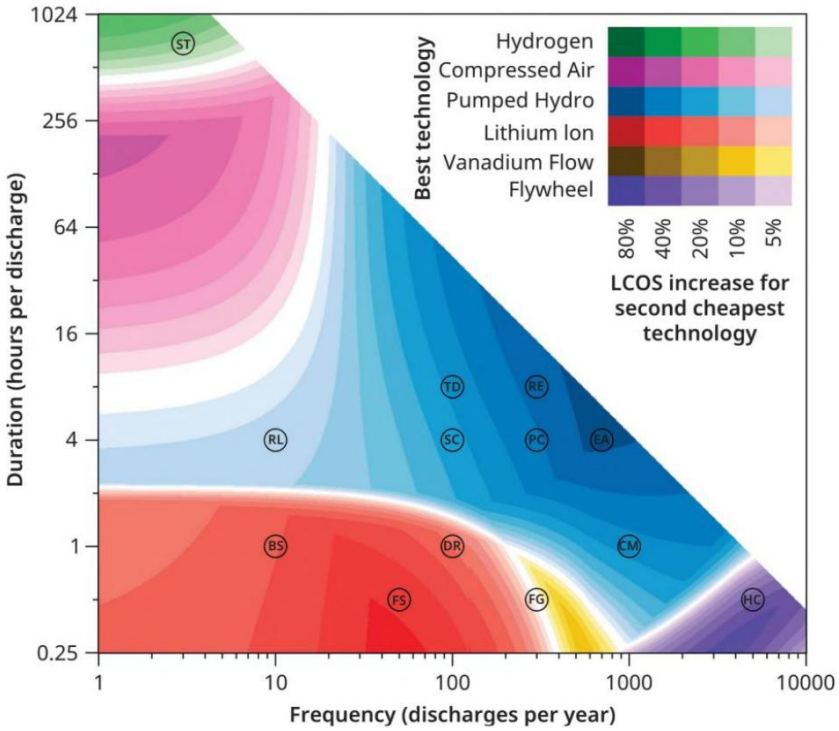

Figure 3: Probabilistic competitive landscape of min-cost storage technologies in 2020 [6]

LCOS rather than ACC is the main metric in this technoeconomic study due to a myriad of factors. Firstly, energy storage technologies were found to exhibit a higher sensitivity to climate factors than power storage technologies, which will be elaborated upon in Section 13. Additionally, the dominant technology borders in energy storage applications are generally less clear than for power applications, as seen in Figure 3. The

methodology for determining the overall impact of climatic factors on LCOS is described in the following section.

7. Methodology

This study aims to quantify the LCOS change and reassess the competitive landscape for ESS in Arctic conditions. In order to achieve this, the key challenges and mitigations associated with Arctic ESS were first identified and compiled. Next, real-world implementations of each storage type, particularly in Arctic regions, were examined in order to contextualise their practical feasibility. The power-consumption processes within each storage system were analysed to assess the possible impact of climate on operating costs. The most climate-sensitive capital costs were identified, such as on-site construction, thermal management system (TMS), and front-end engineering design (FEED) costs. Lastly, any Arctic factors that could affect the lifetime storage dispatch were identified for each technology. A python-based tool was created to quantify the net effects of these climate-driven technoeconomic factors as a function of the following input parameters:

- Output Power
- Discharge duration
- Charges per year
- Discount rate
- Power cost
- Project lifespan
- Wintertime low + mean yearly temperature

Plant winterisation generally involves changes to both CAPEX and OPEX, the latter of which is determined by the climate-induced power consumption. Each storage system has a unique thermal management strategy and requires a customised approach, which will be detailed in Sections 8 through 12.

While the precise impact of Arctic conditions on project construction costs is difficult to quantify, a construction cost guide released by RSmeans in 2023 estimates that civil works projects are approximately 25% costlier in Alaska relative to the US average [60], [61]. On-site construction in the Arctic will be lengthier and more expensive due to narrower weather windows and the heightened costs of shipping, equipment rental, and labour. In this analysis, the 25% location-based adjustment is applied globally and across all storage technologies, though it carries significant uncertainty. For example, a region like Norway which has significant experience with building PHS in remote and extreme conditions will likely have less of a locational markup on construction costs than the USA. Thus, an uncertainty is applied to the locational markup and the resulting effects on LCOS are analysed with a sensitivity study in Section 13.1.

Multiple industry sources estimate that FEED costs equal approximately 30% of the installed plant CAPEX [62], [63]. Thus, the *increase* in FEED costs due to climate-related factors can be estimated as 30% of the *increase* in installed CAPEX.

The baseline CAPEX and OPEX were solved for using the specific-power and specific-energy costs summarised in Table 3. The total CAPEX and OPEX were derived by summing the product of the specific-power cost and the plant's power capacity with the product of the specific-energy cost and the plant's energy

capacity. The origin of these specific-cost values will be discussed in the following section. The climate-induced changes to CAPEX and OPEX were then added to the baseline costs to determine the Arctic project costs. Any climate-induced changes to lifetime storage throughput were summed with the baseline storage as well.

The numerator of the LCOS defined in Equations 1 and 2 combine the CAPEX with the discounted OPEX, charging costs, and replacement costs [64]. Cash discounting calculations depend on the project's discount rate, construction time, lifespan, and replacement intervals. Discounted lifetime storage throughput was also modelled per Equation 4, with provisions for the temporal and cyclic degradation of each technology. The lifetime costs and lifetime storage dispatch were then divided to solve for LCOS [64].

$$(1) \quad LCOS = \frac{Investment\ Cost + \sum_n^N \frac{O\&M\ cost}{(1+r)^{n+T_C}} + \sum_n^N \frac{Charging\ cost}{(1+r)^{n+T_C}}}{\sum_n^N \frac{Elec_{Discharged}}{(1+r)^{n+T_C}}}$$

$$(2) \quad Investment\ Cost = CAPEX + \sum_{rep=1}^{R} \frac{Replacement\ Cost}{(1+r)^{T_C+rep\times T_r}}$$

$$(3) \quad \text{Charging Cost} = \frac{P}{RTE} \cdot CD \cdot CPY \cdot Power\ Cost$$

$$(4) \quad \sum_n^N \frac{Elec_{Discharged}}{(1+r)^n} = P \cdot DD \cdot CPY \cdot DoD \times \left(1 - \eta_{self}\right) \cdot \sum_{n=1}^{N} \frac{\left(1-Cyc_{Deg}\right)^{(n-1)\times CPY}\left(1-T_{deg}\right)^{(n-1)}}{(1+r)^{n+T_C}}$$

Where:

- *r = discount rate*
- *n = years from 1 to N*
- *T_c = construction time*
- *T_r = replacement interval*
- *rep = replacement number*
- *R = total number of replacements*
- *P = output power*
- *DD = discharge duration*
- *CD = charge duration*
- *CPY = charges per year*
- *DoD = depth of discharge*
- *η_{self} = self-discharge between cycles*
- *Cyc_{deg} = degradation per cycle*
- *T_{deg} = temporal degradation per year*

A deterministic, python-based model was developed to compute the baseline and Arctic LCOS for each storage technology using the key inputs of power, discharge duration, charges per year, discount rate, power cost, project lifespan, and reference temperatures. This tool allows the user to compare technology LCOS for an individual project or a wide range of projects with incremental combinations of discharge duration and cycle frequency. Lastly, a branch of this code can apply uncertainties to key climate-related variables in order to assess the possible range of LCOS values for each storage technology. This allows the user to ascertain each technology's economic susceptibility to Arctic climatic factors, and the key cost drivers therein.

It should be noted that the yearly OPEX reported in this study includes charging costs, given that both are assumed to be constant from year to year and are discounted on the same yearly interval. Additionally,

transmission line costs were not included in this calculation of LCOS— though in reality they could be a differentiating factor that favours denser, modular technologies. Lastly, decommissioning costs at end-of-life were assumed to be negligible to the overall LCOS and are thus excluded from this study.

7.1. Data Sources

Table 3 below shows a compendium of technoeconomic parameters for each storage technology as of 2025. These parameters were taken mainly from Schmidt and Staffell's StorageNinja tool, which uses 2020 data from research institutions, industry reports, and interviews [6], [59]. The exception to this is the specific construction costs, which have been compiled on a case-by-case basis. To validate these parameters for 2025, additional sources were consulted, including the NREL 2024 Annual Technology Baseline (ATB) and the PNNL Energy Storage Cost and Performance Database from 2023 [65] [66]. To supplement hydrogen ESS cost data, industry tools such as LCOH+ and the Agora LCOH calculator were used [62], [67]. Similarly for PHS, a 2024 cost model by Cohen et al. was referenced. This model was published through NREL and creates a bottom-up cost breakdown for PHS from Electric Power Research Institute (EPRI) data and other recent PHS proposals [63].

Generally, the StorageNinja values derived from 2020 data are still valid today, with a few notable discrepancies. Cohen et al.'s PHS calculator, which focuses on the USA, has significantly higher cost predictions than StorageNinja [61]. Alternately, the "Cost Base for Hydropower Plants" report from Norway's Water Resources and Energy Directorate estimates significantly lower capital costs [50], [68].

Another discrepancy is that several recent Chinese CAES plants have a lower published CAPEX than Table 3 would have predicted, likely due to the lower EPC costs in that region [69]. PNNL's 2023 CAES data, however, is in family with StorageNinja's specific cost values [66].

Tesla's Megapack has transparent pricing that is approximately 30-40% lower than the StorageNinja prediction for BESS, but this cost does not include installation, tax, or FEED costs [70]. Conversely, the comprehensive cost estimates for utility-scale BESS from NREL's ATB and PNNL's 2023 report are significantly higher than StorageNinja cost parameters [65], [66].

Lastly, PNNL's 2021 data for Hydrogen PGP storage predicts a specific-power cost that is approximately 30% lower than StorageNinja's values [66]. Conversely, the "Agora" LCOH calculator developed by Accenture aligns with StorageNinja in terms of specific-cost predictions [62].

Given the disagreement in recent cost data, StorageNinja's values were chosen as a reasonable average across countries and plant scales for 2025. It should be noted that the CAES specific costs in Table 3 are for diabatic CAES, and the costs associated with the TES system must be added to model adiabatic CAES.

Parameter	BESS	Flywheel	PHS	CAES	Hydrogen
Specific-Power Investment Cost (per kW)	$250.00	$600.00	$1,100.00	$1,300.00	$5,000.00
Specific-Energy Ivestment Cost (per kWh)	$300.00	$3,000.00	$50.00	$40.00	$30.00
Specific-Power OPEX (per kW)	$5.00	$5.00	$20.00	$14.00	$30.00
Specific-Energy OPEX (per MWh)	$0.40	$2.00	$0.40	$2.00	$0.40
Specific Construction Cost	49 USD/kW, 12 USD/kWh	20% CAPEX	479 USD/kW, 19.2 $/kWh	226.4 USD/kW, 21.4 USD/kWh	10% CAPEX
RTE	0.86	0.88	0.80	0.65	0.35
Construction Time	1.00	1.00	3.00	2.00	1.00
Depth of Discharge	0.80	1.00	1.00	1.00	1.00
Self Discharge	0.01	0.10	0.00	0.00	0.00
Cycle Life	3,500	200,000	30,000	15,000	10,000
EoL Threshold	0.80	0.95	0.95	0.95	0.95
Annual Temporal Degradation	0.01	0.00	0.00	0.00	0.00

Table 3: Key Input Parameters for ESS Modelling, shown in 2020 USD

The following sections will deep dive into each technology's modeling approach and assumptions. Each model's results will be presented within the framework of different project scenarios. These scenarios are chosen to highlight key sensitivities within each ESS subtype. Finally, Section 13 will compare the results across all technologies and for a range of conditions. The competitive landscape of ESS in the Arctic will be assessed under uncertainty and the sensitivities to power level, power cost, discount rate, and maintenance risk will be analysed.

8. Battery Energy Storage System (BESS) Modeling

BESS is the most common storage technology deployed in the Arctic today, primarily in the form of lithium-ion or lead acid packs that provide spinning reserve or black start services [1], [45]. These BESS installations must have robust thermal management systems to prevent the degradation modes described in Section 4.2.

Utility-Scale BESS typically consists of a containerised array of battery cells and their corresponding Power Conversion System (PCS), which use an integrated chiller to reject waste heat. Three of the largest commercial BESS modules are Tesla's Megapack 2 XL, CATL's EnerC+, and SAFT's Intensium High Energy. All of these systems use Lithium Iron Phosphate battery technology with liquid water/glycol cooling [46], [70], [71]. In these systems, the liquid coolant circulates through channels in each battery pack's cold plate, absorbing heat before flowing to a condenser and expansion valve, with real-time sensors adjusting flow to prevent thermal runaway and ensure optimal performance. In applications that require

heating, the coolant fluid can bypass the chiller and reroute through resistive heaters to keep cells warm during cold, idle periods. This section will aim to estimate the cost deltas associated with building and operating a BESS in the Arctic, primarily driven by:

- Increased container heating during idle periods
- Reduced cooling loads during operational periods
- The added capital expense of container heaters and insulation
- The added costs of winterising chillers + external fluidic components
- Locational construction costs

8.1. BESS Operating Costs

To assess the impact of climate on BESS operating costs, it is first necessary to estimate the number of containers required to meet a project's power and discharge duration specifications. This is done using the average power rating and volumetric energy density of the Tesla, Saft, and CATL modules mentioned above. The average yearly HVAC demands per container as a function of outside temperature were calculated using thermal parameters from a 2023 paper on the impact of heating and cooling loads on BESS in extreme cold climates [72]. The nominal thermal resistance of each container was first quantified, and a sensitivity study was conducted on the ideal insulation thickness to reduce lifetime thermal management costs. In Figure 4, a wintertime low of -40°C and a mean yearly temperature of -10°C were used for reference. Under these conditions, adding insulation to the BESS containers improves the lifetime cost. The ideal thickness is sensitive to assumptions on the regional power cost and the utilisation profile, the latter of which can be estimated from the discharge duration and the charges per year. The plot to the left represents a scenario with frequent utilisation and inexpensive power prices, whereas the right plot represents an opposite scenario with infrequent utilisation and expensive utility rates. In the left plot, less insulation is needed to reduce overall costs, and insulation thickness beyond 0.10 m just adds to the overall cost. In the right plot, the expensive heating costs and the long idle periods make an insulation thickness of 0.18 m the ideal solution. Going forward, a nominal insulation thickness of 0.125 m was assumed as a compromise across the possible range of project conditions.

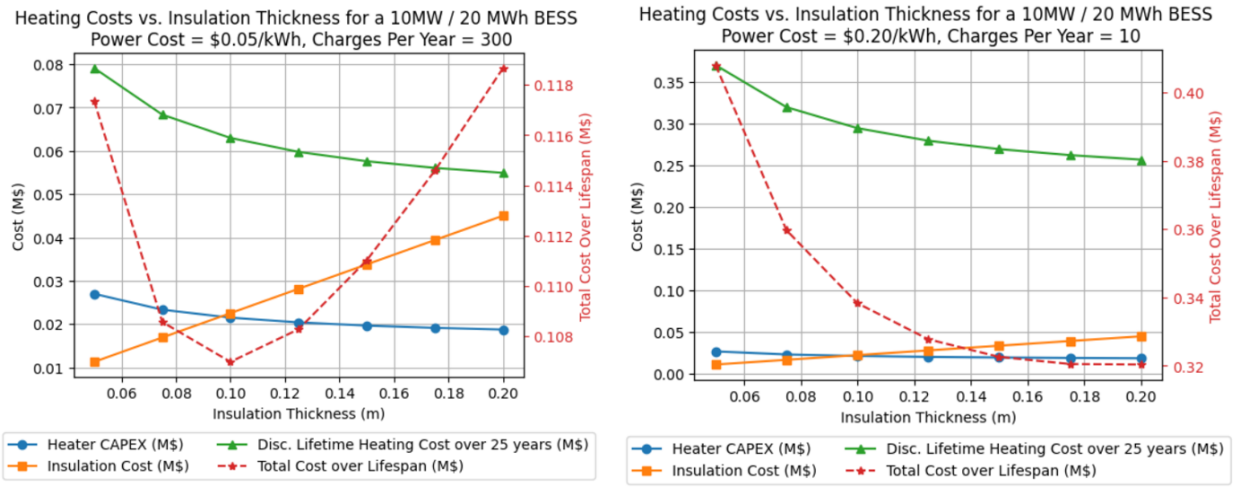

Figure 4: Insulation Thickness Sensitivity Study, BESS

Given the common inputs of mean yearly temperature, power output, discharge duration, cycling frequency, power cost, and discount rate, the total heating cost required to maintain all containers at or above 15°C during idle periods is estimated. This 15°C threshold was carried over from Olis et al.'s analysis of BESS in extreme cold climates [72]. The thermal resistance of each container plus the thermal resistance of the insulation are summed to find an effective resistance. The average heat input is then calculated by dividing the temperature delta between the desired indoor temperature and average outdoor temperature by the thermal resistance of the container and the heat exchanger efficiency. The simplified calculation in Equation 5 below assumes perfect thermal coupling between the insulation surface and ambient air, which is a reasonable approximation in steady-state conditions. The capital cost of heaters is calculated using the same methodology, but solving for the peak power demand at the wintertime low temperature of -40°C. This peak power load is multiplied by the specific capital cost of resistive heaters (0.50 USD/W) and the number of containers to estimate the overall heater costs. The insulation and heater costs are treated as added costs (i.e. mild-climate BESS do not need any heaters or insulation), which is likely conservative.

$$\Delta OPEX_{heating} \simeq \left(\frac{15°C - mean\ yearly\ temp}{Resistance_{th,container} \times \eta_{HEx}} \right) \cdot yearly\ idle\ period \cdot Power\ cost \cdot number\ of\ containers \quad (5)$$

The next component of OPEX to consider is the cooling power required during operational periods. It is assumed that the nominal roundtrip efficiency of BESS is 86%, and that all inefficiency manifests as waste heat, which is reasonable in cases where the Power Conversion System is containerised alongside the cells [72]. Since most BESS employ a liquid cooling circuit and an integrated chiller, the input power required to expel the operational waste heat can be estimated using the COP of the chiller. The COP of an air-cooled chiller varies with temperature in a parabolic trend and generally improves at lower air temperatures [73]. Thus, the cooling cost savings in the Arctic should be proportional to the difference between inverse COP at each reference temperature per Equation 6.

$$\Delta OPEX_{cooling} \simeq \frac{P}{RTE} \cdot (1 - RTE) \cdot \left(\frac{1}{COP_{hot}} - \frac{1}{COP_{cold}} \right) \cdot yearly\ operational\ period \cdot Power\ cost \quad (6)$$

The yearly operational period can be inferred from the system's charges per year and discharge duration, and the waste heat is calculated as a function of power and RTE in Equation 6 above. It is assumed that no significant cooling is needed during idle periods in the Arctic.

8.2. BESS Capital Costs

Some of the cost factors associated with building BESS in an Arctic location were indirectly calculated through the operating costs, such as heater and insulation CAPEX. The remaining climate-driven factors include the locational markup of construction work and the winterisation of the chiller system. Commercially-available BESS are typically rated down to -20°C, with the TMS system as the limiting factor [46], [70], [71]. As mentioned previously, the TMS uses a pumped coolant to reject waste heat from the cells and PCS through an air-cooled chiller. Winterisation of the chiller system could involve switching to a specialty coolant, cold-rated fluidic components, additional heaters, or even sourcing an entirely new chiller. The cost associated with this winterisation was estimated as an extra 15% of the baseline chiller

system cost, which can be approximated as 130 USD/kW_{th} [74]. An uncertainty analysis on this and other key assumptions are analysed in Section 13.1.

After estimating the winterisation cost of the chiller system, the model quantifies the construction costs based on data from NREL's *Utility-Scale Battery Storage ATB* 2024 report and applies the 25% locational markup as discussed in the Methodology section. The specific construction costs used in this study are summarised in Table 3. Generally, the on-site construction costs are less consequential for BESS as compared with other technologies, due to its modular and pre-fabricated nature.

8.3. Net Effects on LCOS

The additional OPEX and CAPEX outlined above ensure that the BESS is kept within its rated operating conditions despite the extreme environment. Thus, there should be no performance degradation due to climate factors in this case. With the proper TMS design, the total storage dispatched by BESS should be the same for a given supply and demand profile, regardless of climate.

The key cost drivers for LCOS are displayed below for three scenarios, in order to illustrate the relative influence of each climate cost factor. The first scenario represents a small BESS with expensive power prices and infrequent usage, which is most representative of historical batteries in the Arctic. In this scenario, the factors in order of their influence are construction cost markups, OPEX change, winterised chiller costs, heater & insulation costs, and finally the added overhead costs. Scenario #2 is a high-power BESS with frequent usage and cheap power prices, which represents an ESS that provides multiple grid services in a larger grid system. In this scenario, the construction cost dominates the LCOS change and OPEX is less significant, primarily due to the low power cost. In this case, OPEX contributes a *negative* change to LCOS because the scenario's high utilisation means that the saved cooling costs during operation outweigh the added heating costs during idle periods. Lastly, Scenario #3 is similar to Scenario #2 but with a longer discharge duration of six hours. In this scenario, the total dispatched storage is at its highest and LCOS is at its lowest. The additional cost of construction is nearly cancelled out by the saved operational cooling costs, and thus climate effects in this scenario are very low.

	Relative Contribution to LCOS Change (%)		
Cost Factor	Scenario 1	Scenario 2	Scenario 3
Construction Cost	41.1%	47.9%	38.8%
Heater & Insulation Cost	9.0%	10.5%	16.7%
Custom Chiller Cost	7.8%	9.1%	6.2%
FEED Cost Increase	5.0%	5.9%	4.1%
OPEX Change(disc.)	37.2%	26.6%	34.3%
Temperate LCOS per kWh	$6.71	$0.36	$0.31
Arctic LCOS per kWh	$7.05	$0.37	$0.31
Total LCOS Change Due to Climate (%)	5.1%	0.8%	0.3%

Table 4: Contribution to LCOS Change in Arctic BESS. Scenario 1: 10 MW/1.5hrs, powercost = 0.20 USD/kWh, CPY = 10. Scenario 2: 100 MW/1.5hrs, powercost = 0.05 USD/kWh, CPY = 1000. Scenario 3: 100 MW/6hrs, powercost = 0.05 USD/kWh, CPY = 600

The table above shows that construction is the single most significant factor affecting Arctic LCOS change—even for a modular technology like BESS. The OPEX change due to increased heating and decreased cooling demand is significant as well, but the net change is highly dependent on a project's operational-to-idle ratio. From this, it can be concluded that batteries with less utilisation and higher power prices are more economically affected by an Arctic climate, but generally the climate effects on LCOS are relatively minor.

9. Flywheel Cost Modeling

This section analyzes the added costs associated with building a Flywheel Energy Storage System (FESS) in the Arctic. As explained previously, a flywheel module consists of rotor and stator assemblies. A vacuum is maintained within the structural housing to reduce aerodynamic drag on the flywheel, which provides an effective thermal isolation between the two subassemblies. Flywheels have an excellent RTE but there are still losses, particularly in the bearings and motor windings, which will create excess heat that must be actively managed. Flywheel TMS often takes the form of a pumped coolant loop which removes heat from the power electronics and the flywheel "stator water jacket" via an air-cooled condenser. The stator water jacket consists of coolant channels integral to the stator housing in the vicinity of the motor windings, where heat generation is highest [75]. Large-scale flywheel systems are commonly rated for full-power operation from at least -20°C to 40°C and thus require less thermal management than BESS [29], [76]. While there are very few examples of FESS the Arctic, it can be inferred that the TMS could be adapted for extreme cold operation with the addition of resistive heaters to the coolant circuit and a lower freezing point coolant. Alternatively, depending on the design limitation, the flywheel module could avoid the need for heaters altogether by changing to a low-temperature bearing grease and/or adjusting design clearances to account for the aggravated thermal expansion mismatch.

In large FESS installations, roughly every ten modules share a container that houses the shared power conditioning and control electronics, thermal management system, vacuum pumps, and other auxiliary equipment [76], [77]. These containers will require insulation and heating during idle periods as well.

Flywheel's high power density, modular nature, and broad temperature rating make it an inherently robust choice for all climates. The cold-temperature effects listed below will be investigated in order to determine their net effects on LCOS.

- Added heaters and insulation for flywheel modules and auxiliary containers
- Saved cooling power
- Increased heating power
- Winterisation of chillers
- Locational factors such as labor, equipment rental, and materials cost

9.1. Flywheel Operating Costs

The methods for calculating the heating costs as well as the saved cooling costs are largely carried over from BESS, since the TMS architecture is very similar. A simple model was built to predict the heat input required to keep FESS above -20°C as a function of the winter low temperature using average values for

volumetric power density, energy density, and module power. This is a conservative analysis, given that flywheels can likely be stored at temperatures lower than -20°C and would only need heating prior to operation. The number of flywheel modules was solved for using the average power and energy ratings of commercially-available FESS. While there are companies such as CHN Energy and Piller Powerbridge that offer flywheel modules up to 4 MW, the nominal module size is assumed to be 250 kW, which is in family with FESS plants that are currently operational [77], [78]. With such a low thermal limit of -20°C, heating costs even in the coldest climates are low as compared with BESS. The cooling power savings are comparable to that of BESS, given that both technologies have similar RTEs and chiller systems.

The baseline OPEX is calculated using the specific cost values shown in Table 3 and augmented with the operating cost outputs from this model to calculate the Arctic OPEX. The resulting change is summarised in the context of other climate cost factors in Section 9.3.

9.2. Flywheel Capital Costs

Just as with the other storage technologies in the Arctic, construction cost will play a major role in climate-related changes to LCOS. There is very little public data on the construction costs of installing FESS. It may have similar costs to BESS, given that both systems share a modular architecture. However, FESS likely has higher construction costs due to its larger land footprint and the need for leveled, partially-submerged foundations [76], [79]. It is common for FESS foundations to be partially underground because of the natural containment benefits in the event of a high-speed rotor failure, as well as the superior vibration characteristics. A PNNL publication from 2019 estimates that flywheel construction costs comprise 20% of the baseline CAPEX, so that is the metric used to calculate construction costs in Table 3 [80]. The result is that FESS construction costs are over double that of BESS, with the same locational markup of 25% applied. Construction cost uncertainty will be further examined in Section 13.1.

9.3. Net Effect on LCOS

Flywheels become competitive at high cycle frequencies due to their long cycle lives and the avoided replacement costs that a similar BESS would face. The wide temperature window and relatively narrow range of applications of FESS as compared with BESS makes flywheels less impacted by cold-climate factors overall. They require minimal thermal management and operate over short discharge durations—resulting in lower energy-specific construction costs—and therefore show the least sensitivity to Arctic climate among all storage technologies examined in this review.

	Relative Contribution to LCOS Change (%)	
Cost Factor	Scenario 1	Scenario 2
Construction Cost	83.07%	72.74%
Heater & Insulation Cost	3.98%	2.52%
Custom Chiller Cost	3.27%	1.84%
FEED Cost Increase	2.17%	1.31%
OPEX Change (disc.)	7.51%	21.58%
Temperate LCOS per kWh	$0.83	$0.13
Arctic LCOS per kWh	$0.86	$0.13
Total LCOS Change Due to Climate (%)	3.26%	1.54%

Table 5: Contribution to LCOS Change in Arctic FESS Plants. Scenario 1: 10 MW/0.25hrs, powercost = 0.20 USD/kWh, CPY = 1000. Scenario 2: 10 MW/0.5hrs, powercost = 0.05 USD/kWh, CPY = 8000.

Two scenarios were analysed in the Table above: Scenario 1, which involves infrequent usage and high power costs, and Scenario 2, which involves high utilisation and low power costs. Unsurprisingly, the LCOS is significantly better in Scenario 2, where the amount of dispatched storage is highest and the charging cost is lowest. In both scenarios, the OPEX of Arctic FESS decreases due to the saved cooling costs, though not enough to outweigh the locational construction costs.

10. Pumped Hydro Storage (PHS) Modeling

PHS can be an attractive option where there is suitable terrain and, ideally, existing hydroelectric infrastructure. However, icing will need to be actively managed for any PHS plant in the Arctic.

A 2013 review of ice effects on hydropower by Gebre et al. details the impact of cold climate on PHS, and various mitigation strategies [81]. Cold climate can reduce energy capacity, roundtrip efficiency, and power rating of a PHS plant. Ice formation on the lower reservoir represents an energy capacity reduction, since less liquid water is available to "charge" the storage system. Ice growth on the upper reservoir represents a roundtrip efficiency loss, seeing as some of the water that was pumped to a higher energy state has frozen and can no longer be discharged through a turbine to produce power. And lastly, any ice blockage in the waterways (most commonly at the filters, which are called "trash racks") will result in reduced power output. Frazil ice is a common issue in cold-weather PHS, and it takes the form of loose crystals in supercooled turbulent water which can adhere to one another and cause blockages at the trash racks, sometimes resulting in a complete shutdown of the plant [81].

Various strategies are employed to manage cold climate risks in pumped hydro systems. Designing the penstock and power station to be underground is common practice in high-latitude PHS [50]. While it's impractical to heat an entire reservoir of water, deeper reservoirs with a smaller surface-area-to-volume ratio will see less energy capacity reduction. The ice layer will grow as air temperatures drop below freezing and provide some insulation for the water below. However, draining or filling the reservoirs will cause the ice layer to break apart into fragments which can then cause blockages or even damage the turbine if they

get past the trash racks. Thus, submerging the trash racks well below the freezing level of the reservoir is best practice. Common methods to prevent ice blockage at the trash racks are mechanical raking, compressed air, and active heating. Manual clearing using a raking mechanism is the most common historically, but comes with increased maintenance and more mechanical failure points [81]. A bubbler system, on the other hand, uses compressed air to recirculate deeper, warmer water over the bars of the trash rack to clear ice. This option is relatively cheap and low energy, provided the water level never drains below the top of the trash rack. Lastly, active heating of the trash rack crossbeams is energy-intensive but effective at all water levels [81].

This section will evaluate the cost effects of building PHS in the Arctic as compared with a temperate climate. These costs are associated with:

- Ice blockage prevention (via mechanical rakes, compressed air, or active heating systems)
- Underground power station
- Locational factors such as labor, equipment rental, and materials cost
- Energy Capacity reduction as a result of ice layer formation

10.1. PHS Operating Costs

As discussed previously, the power capacity can be significantly diminished due to ice blockages. A turbine's hydrodynamic power output is defined as the product of fluid density, head height, volumetric flowrate, gravitational constant, and turbine efficiency. Blockages in bottleneck areas such as the trash racks will reduce the water flowrate and thus proportionally affect the output power of the plant.

Instead of modeling the net power loss associated with blockages, this study employs the strategy of estimating the system costs associated with eliminating ice blockages altogether via active heating at the bottlenecks. The active heating approach was chosen for its ability to remove ice remotely (unlike manual raking) and for its effectiveness at all water levels (unlike a bubbler system). A thermodynamic model calculates the heat input required to maintain both the upper and lower trash rack beams at 5°C when exposed to an incident crossflow at 0°C and 6 m/s. These parameters were conservatively chosen, as the incident water temperature is just over freezing and a flow velocity of 6 m/s is cited by NREL's PHS modeling tool as the maximum tunnel flow velocity [63]. It can be assumed that the trash rack beams are hollow, and that heat is applied to the inner surface of the beam either via resistive heaters or a ground source heat pump. The trash rack geometric parameters are calculated for a maximum allowable head loss using Meusberger et al.'s equation 7 below [82]. This model solves for the minimum crossbar spacing to not exceed a head loss of 1% using the bar length, which is derived from the mass flowrate and flow velocity— as well as the bar diameter, which is defined as a fixed proportion of the bar length.

$$\Delta h = K \cdot p^{1.33} \left(\frac{b}{l}\right)^{-0.43} \frac{V^2}{2g} \sin\theta \tag{7}$$

Where:

- Δh *= head loss*
- K *= form factor (2.42)*
- p *= blockage ratio (cross-sectional blockage area / cross-sectional tunnel area)*

- *b = clear spacing between bars (m)*
- *l = length of bars (m)*
- *V = flow velocity upstream of trash rack*
- *θ = vertical angle between flow direction and trash rack (60°)*

The model then uses the Churchill-Bernstein correlation to calculate the Nusselt number of a cylinder in turbulent crossflow [83]. The convection coefficient is derived from the Nusselt number and the convective heat loss of each crossbeam is calculated and summed using equations 8 through 10 below.

$$(8) \quad Nu_D = 0.3 + \frac{0.62 Re_D^{0.5} Pr^{0.333}}{\left(1+\left(\frac{0.4}{Pr}\right)^{0.667}\right)^{0.25}} \cdot \left(1 + \left(\frac{Re_D}{282000}\right)^{0.625}\right)^{0.8}$$

$$(9) \quad h = \frac{Nu_D k}{D}$$

$$(10) \quad Q = \frac{hA_s\,(T_{bar} - T_{water})}{\eta_{HEx}} \cdot n_{bars}$$

Where:

- $Re_D = \frac{VD}{\nu}$
- $\mathrm{Pr} = \frac{c_p \mu}{k}$
- *k = thermal conductivity*
- *D = trash rack bar diameter*
- *Q = required heat input*
- *A_s = surface area per bar*
- *n_{bars} = number of bars per trash rack*

It was found that resistive heaters will be less expensive overall than a ground source heat pump option—even when assuming a high utility rate, a long project lifespan, and the lower efficiency of resistive heating. This is due to the capital costs of a ground source heat pump, which are approximately five times higher than an equivalent resistive heater [84]. The peak heater power and the specific capital cost of resistive heaters are thus multiplied to estimate the total cost of the trash rack heaters. The annual operational cost is then calculated from the cycle frequency, duration, and power cost, assuming that active heating is needed during charging or discharging operations for approximately half of each year.

The heaters will only be activated during or shortly before the charge or discharge of the PHS, and can thus be termed as an effective RTE loss. The RTE losses due to trash rack heating as well as the capacity reduction due to ice formation are plotted versus the outside air temperature in Figure 5 below. The RTE loss due to heating correlates with the plant power rating, which determines tunnel diameter and, indirectly, the trash rack geometry. The RTE loss due to ice formation correlates to the reservoir aspect ratio, snow depth, and the cycling frequency. The icing calculations and their impact on LCOS will be further elaborated upon in Section 10.3.

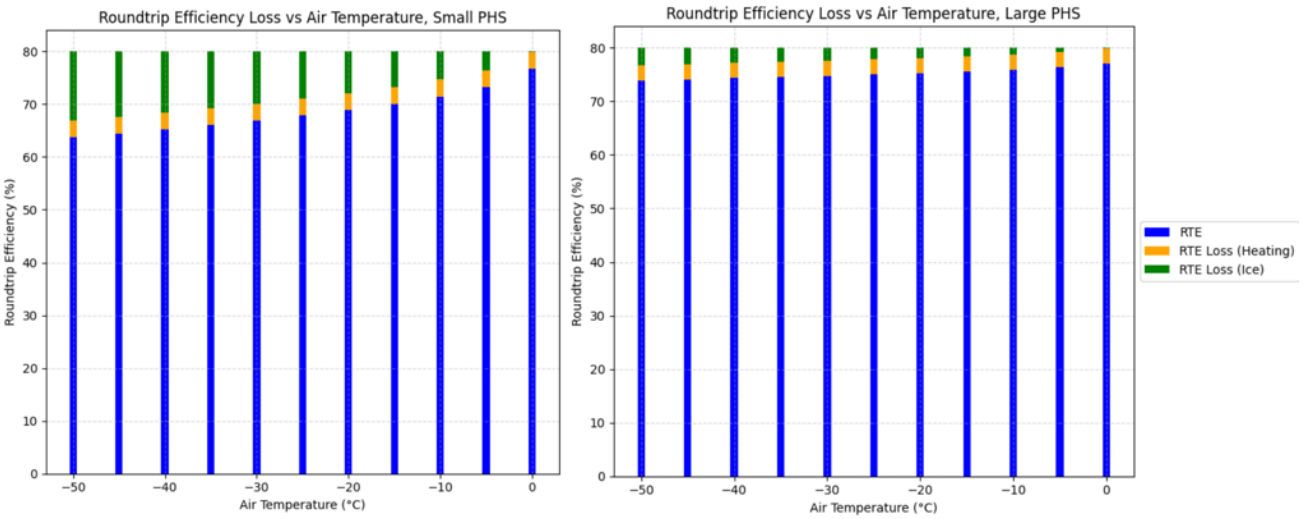

Figure 5: PHS efficiency losses due to heating and icing. Common assumptions: 10 charges per year, AR = 50. Small PHS: 90 MW/10hr. Large PHS: 1 GW/18.5hr

10.2. PHS Capital Costs

PHS is inherently bespoke and thus capital costs will fluctuate greatly depending on the constraints of each site. A 2024 NREL tool by Cohen et al. itemises the capital costs of small and large PHS plants in great detail [63]. Generally, the components of CAPEX which are most sensitive to climate factors are the thermal management system and the on-site construction costs. The heater CAPEX has been indirectly calculated in Section 10.1, and now it becomes necessary to isolate the construction costs associated with building PHS power stations, water conductors, and dams in an Arctic climate. Power station and water conductor construction costs generally trend with power level, while dam and reservoir costs trend with energy capacity. Though each project will have its own unique regulatory and geological conditions which will also affect the overall costs. The specific construction cost metrics listed in Table 3 represent simplified averages across common PHS plant scales, derived from Cohen et al.'s cost model. Additionally, according to this US-focused cost model, there is a construction cost delta of approximately 115 million USD associated with moving the power station underground, which is fairly insensitive to plant scale [63]. This is mainly because of the additional operations required to create the access tunnels, draft tubes, and tailrace tunnels, which wouldn't be needed in surface power stations [63]. However, the Norwegian Water Resources and Energy Directorate estimates a much lower and more variable cost for underground power station development, which averages to approximately 19 million USD across the same scale [68]. Thus, the "fixed" cost associated with building an underground power station was approximated by averaging these two values, which comes to 67 million USD. A large uncertainty has been applied to this value and will be discussed further in Section 13.1.

10.3. Net Effect on LCOS

Storage capacity and RTE are reduced during the winter months due to ice formation. The amount of performance loss is dependent primarily on the reservoir aspect ratio, the usage frequency, the outside temperature, and the snow cover [85]. Ice layer growth was modeled as a function of time using the Stefan equation shown below, which balances the heat loss due to conduction through the ice with the latent heat

of fusion created during ice formation [85]. This equation assumes that the top surface of the ice is equal to the air temperature and the bottom surface is equal to the melting point, 0C. Note that the reservoir dimensions will not affect the estimated ice thickness under this approach, since a homogenous temperature of 0C at the water-ice interface is assumed. This is a reasonable assumption for most Arctic lakes that rarely get above 5°C, but can be conservative in cases where the reservoir has good circulation and warmer depths. A slight modification was made to include the insulating effects of snow, which recalculates the ice surface temperature based on snow cover using the Equation 12 and substituting Ts* into the Stefan equation [85].

$$\frac{dh_i}{dt} = \frac{k_i}{\rho_i \cdot L_f \cdot h_i}(T_m - T_s^*) \quad (11)$$

$$T_s^* = \frac{h_s \cdot T_m + r \cdot h_i \cdot T_a}{h_s + r \cdot h_i} \quad (12)$$

Where:

- h_i = *ice thickness*
- h_s = *snow depth*
- T_m = *melting point*
- T_a = *air temperature*
- r = *thermal conductivity ratio* (k_s/k_i)
- L_f = *latent heat of fusion*

Given the cycling frequency and duration, the average idle time between charges is calculated. Using the mean yearly temperature, which is below freezing in most Arctic regions, the annual capacity loss due to ice formation can be estimated. The sensitivity of energy capacity loss to reservoir aspect ratio and snow cover are displayed in Figure 6 below. The reservoirs are modeled as spherical caps, where the aspect ratio is equal to the radius of curvature over the depth, and AR = 1 signifies a hemispherical reservoir. The volume of the upper reservoir is estimated by integrating the maximum volumetric flowrate of water over the discharge duration, assuming a usable fraction of 85% [63]. The growth in ice thickness between charges is multiplied by the reservoir surface area to estimate the average capacity loss per charge cycle. The snow adds a layer of insulation which raises the surface temperature of the ice to Ts*, calculated via Equation 12. As expected, the capacity loss is most significant for shallow reservoirs with no snow cover under long periods of stagnation and shows more sensitivity to aspect ratio than to snow cover.

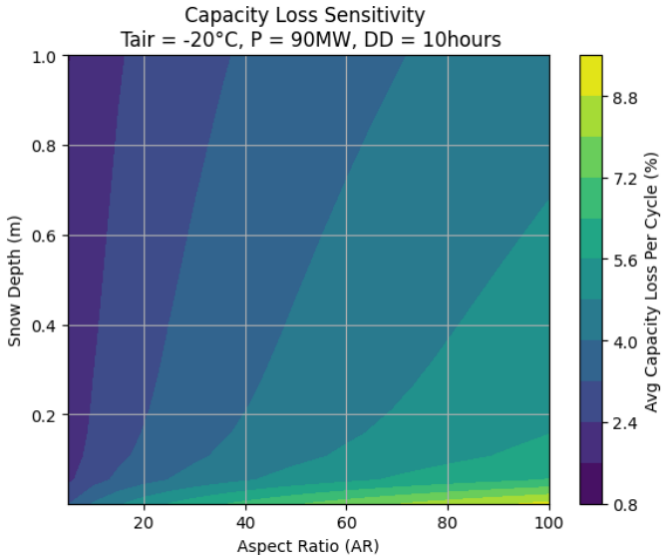

Figure 6: PHS capacity loss due to icing as a function of aspect ratio and snow cover

For the purposes of this study, a nominal aspect ratio of 50:1 and a mean winter snow depth of 0.5m were assumed in the calculation of capacity loss. There are elements of both conservatism and optimism in the capacity reduction calculation. Using Stefan's equation to calculate ice growth is conservative because it assumes no reservoir circulation. Conversely, the assumption that the ice layer breaks up and melts when the reservoir drains and refills between cycles is optimistic. Thus, the actual reduction in storage capacity for a given mean winter temperature is somewhat uncertain. The assignment of uncertainties to key parameters such as the reservoir aspect ratio and the snow depth help to bound the storage capacity loss, and will be covered in Section 13.1.

Overall, it can be seen from Table 6 that climate has a large effect on PHS system costs—particularly for smaller PHS plants. Three scenarios were analysed to illustrate climate-related effects on LCOS. Scenario 1 is a smaller PHS plant with 10 charge cycles per year and a high power cost. Scenario 2 is a large PHS with a higher cycle frequency than Scenario 1. Scenario 3 uses the same large plant from Scenario 2 but with a low power cost. As expected, the LCOS decreases with power cost and with increased plant scale and utilisation.

As seen in Table 6, the locational markup associated with PHS' high construction costs is the key driver of LCOS increase in Arctic environments. Scenario 1 has a high power cost, but due to infrequent utilisation, OPEX-driven changes are minor. In scenario 2, where utilisation and power costs are both high, the model selects a ground source heat pump over resistive heaters as the most economical option, and thus heater CAPEX plays a more significant role in the LCOS change. Scenario 3 has the lowest LCOS because of its large capacity and frequent dispatches. The storage loss in scenario 3 is the lowest, due to shorter stagnation time between charges. Operational heating becomes more significant in Scenarios 2 and 3 because, unlike other storage technologies, PHS requires heating during operation and these scenarios have the highest utilisation. However, unlike Scenario 2, the low power cost of Scenario 3 enables the use of resistive heaters.

	Relative Contribution to LCOS Change (%)		
Cost Factor	Scenario 1	Scenario 2	Scenario 3
Construction Cost	88.71%	84.05%	93.54%
Heater Costs	0.50%	7.53%	1.20%
FEED costs	0.15%	2.26%	0.36%
Operational Heating Cost (disc.)	0.21%	5.57%	4.64%
Reduced Storage Capacity (disc.)	10.43%	0.60%	0.26%
Temperate LCOS per kWh	$2.13	$0.33	$0.13
Arctic LCOS per kWh	$3.29	$0.34	$0.14
LCOS Change Due to Climate (%)	54.31%	3.25%	7.94%

Table 6: Relative Contribution to LCOS Change in Arctic PHS Plants. Scenario 1: Power = 90 MW/10hrs, Power Cost = 0.2 USD/kWh, CPY = 10. Scenario 2: Power = 1000 MW/ 18.5hr, Power Cost = 0.2 USD/kWh, CPY = 200. Scenario 3, Power = 1000 MW/ 18.5hr, Power Cost = 0.05 USD/kWh, CPY = 200.

The impact of Arctic climate on LCOS varies from 3% to 54% in these three scenarios, illustrating the project-specific nature of climate-driven costs. Smaller PHS plants will be most economically affected by Arctic climate factors, mainly due to the high fixed cost of building an underground station and the larger proportion of capacity loss due to icing, as seen in Figure 5. PHS plants with low utilisation also have a greater sensitivity to climate factors, due to greater ice accumulation between charge cycles.

11. Compressed Air Energy Storage (CAES) Modeling

This section analyzes the added costs associated with building a CAES system in the Arctic. Only Adiabatic CAES is considered in this study due to its low emissions, low marginal cost, and high RTE as compared with Diabatic CAES. There are very few datapoints from which to model Adiabatic CAES, so Diabatic cost models are used and combined with TES and heat exchanger costs to formulate the overall LCOS. Available data from existing projects along with proposals from Siemens have been aggregated to quantify the energy and power-specific costs of commissioning a CAES system. The cold-temperature effects listed below are investigated to determine their net effects on LCOS.

- Change in compressor power
- Increased heating for the powertrain enclosure
- Added insulation for the TES and powertrain enclosure
- Locational factors such as labor, equipment rental, and materials cost
- Energy capacity change at cold temperatures

11.1. CAES Operating Costs

To quantify how CAES operating costs vary with climate, it is necessary to develop a thermodynamic model to capture the fundamental performance dependencies of the system. The working fluid of air is modeled through its compression and expansion processes using the CoolProps extension of python. CoolProps is a widely-used open-source library of thermophysical properties [86].

Multi-stage compression was modeled with a compressor efficiency of 85% and an ideal pressure ratio of 3:1. The internal energy change (ΔU) of air during each stage of the compression process is calculated with CoolProps and 90% is extracted and stored within the TES. The thermal energy is stored in the form of sensible heat, with the same specific cost parameters as assumed in Yang et al.'s 2021 technoeconomic assessment [34]. The temporal TES losses are assumed to be 0.5% per day and the average storage duration can be inferred from the discharge duration and the charges per year.

Depending on the storage pressure and the number of expansion stages, which is calculated using an ideal expansion pressure ratio of 8:1, the remaining stored heat is evenly divided and recuperated at each turbine inlet. In this case, the air storage pressure is assumed to be 70bar, which results in three compression stages and two expansion stages. The total enthalpy change across the turbines is then calculated using CoolProps and the mass flowrate required to achieve a specified output power is derived using the relationship $P = \dot{m} \times \Delta h$. The mass flowrate is then used to calculate the input power with the same equation but using the enthalpy change across the *compressor*. Finally, the RTE can be derived as a function of initial air temperature by dividing the turbine output power with the compressor input power.

From this model, it was found that higher mass flowrates are required at lower ambient temperatures to achieve the same output power. This is supported by equation 13, which shows that a lower turbine inlet temperature results in lower turbine power for a fixed pressure ratio and mass flowrate. Thus, a higher air flow rate is required to achieve the same turbine output power at cold temperatures. This results in a net increase in compressor power and a slight decrease in RTE at colder ambient temperatures, as seen in Table 8.

In an idealised scenario with perfect gas properties, the RTE ($w_{turbine}/w_{compressor}$) would not change with ambient temperature [21]. This is because a cycle with isentropic compression and zero heat losses would result in a constant ratio between turbine inlet temperature (T_3) and compressor inlet temperature (T_1). However, modeling the process using real gas properties through CoolProps indicates that the loss in turbine power at cold temperatures outweighs the savings in compressor power. This conclusion aligns with a more in-depth 2022 study that models a constant-power adiabatic CAES process at varying ambient temperatures [87]. Economically, this reduction in RTE manifests as a higher yearly "charging cost" for Arctic CAES.

$$w_{turbine} = \frac{\gamma-1}{\gamma}\,\dot{m} \times R \times T_3 \times \left[\left(\frac{p_4}{p_3}\right)^{\frac{\gamma-1}{\gamma}} - 1\right] \times \eta_{turbine} \quad (13)$$

$$w_{compressor} = \left(\frac{\gamma-1}{\gamma}\right)\dot{m} \times R \times T_1 \times \frac{\left[\left(\frac{p_2}{p_1}\right)^{\frac{\gamma-1}{\gamma}} - 1\right]}{\eta_{compressor}} \quad (14)$$

A secondary contributor to OPEX is the increased heating demand, particularly during idle periods. Unlike other ESS, there is very little "waste heat" in adiabatic CAES, since the heat generated during compression must be extracted and stored for later use. Thus, any increase in heating demand will need to be bought at the utility rate. Active heating is mainly limited to the powertrain enclosure. The powertrain enclosure shelters the compressor and turbine assemblies from the elements. These large turbomachines generally have a lower thermal limit ranging from -40°C to 0°C and may require heating during the colder months [88]. Since it is common practice to shield large turbomachinery from the elements with a powertrain enclosure regardless of climate, the added costs in this case would be the heating and insulation required to keep the compressors and turbines above an assumed threshold of -10°C. The powertrain enclosure volume can vary significantly depending on the plant layout, but datapoints from Siemens and Goderich CAES layouts were used to approximate the appropriate enclosure size as a function of output power [89], [90]. The insulation and heater power required to maintain this enclosure volume above -10°C were then optimised using the common inputs for outside temperature and heater/insulation cost. Just as with other storage technologies, the baseline OPEX cost was calculated using the parameters from Table 3. The cost deltas associated with higher compressor power and enclosure heating levels were added to the baseline OPEX in order to estimate the Arctic operating costs. An uncertainty analysis on key assumptions from this section is covered in 13.1.

11.2. CAES Capital Costs

Similar to PHS, the main difference between building CAES in the Arctic versus a more temperate and accessible location is the heightened construction costs, particularly those associated with building the TES

and compressed air storage caverns [91]. While there are some salt caverns, aquifers, and hard rock caverns suitable for CAES in the Arctic, any excavation or sealing work required to adapt these geological formations for CAES will be significantly more difficult [33].

The power- and energy-specific construction costs have been aggregated for multiple proposed and real CAES plants as shown in Table 7. The specific construction costs were averaged over a number of sources with wide variation, including both diabatic and adiabatic datapoints. Just as with the other storage technologies, it is assumed that Arctic construction costs are 25% higher than the average baseline. Thus, the additional construction cost associated with building CAES in the Arctic is calculated using equation 15 below.

$$\Delta Cost_{const} = \left(226.4\frac{USD}{kW} \cdot P + 21.4\frac{USD}{kWh} \cdot P \cdot DD\right) \times LocationalMarkup \quad (15)$$

Source	Specific Power Construction Cost ($/kW)	Specific Energy Construction Cost ($/kWh)
McIntosh Plant, Wright 2012	$323.00	$4.00
Black & Veatch, 2012	-	$29.00
Siemens, 2021	$75.00	-
Baillie, 2020	$281.25	$25.40
Matos et al, 2023	-	$8.75
Schmidt & Staffel, 2023	-	$40.00
Average (2020 USD)	**$226.42**	**$21.43**

Table 7: Construction Cost Estimates for various real or conceptual CAES plants

In addition to construction costs, the TES system will require better thermal isolation as compared with that of a temperate environment. Assuming that the TES is designed for similar storage temperatures as a sensible TES in a milder climate, the additional insulation cost required to match the average heat loss is calculated as a function of thermal storage capacity and mean yearly temperature. The TES tank volume and overall cost is estimated using curve fits of the energy density and specific cost data from Yang et al.'s 2021 study on sensible thermal energy storage, assuming a storage temperature of 90°C [34]. An uncertainty study on these TES parameters is conducted in Section 13.1.

The heaters and insulation required for the powertrain enclosure also add to the CAPEX but were found to be insignificant due to the minimal heating requirements. The relative contribution of CAPEX to overall LCOS change of Arctic CAES can be seen in Table 8.

11.3. Net effect on the LCOS

The density of compressed air increases as ambient temperature decreases. Assuming ideal gas properties, the density of air is ~20% higher at -20°C versus 20°C, assuming a storage pressure of 70bar. However, the thermal storage capacity becomes the limiting factor as it will experience greater heat loss at colder temperatures. Additionally, CAES is most cost-competitive when used in conjunction with underground

caverns, and the caverns provide more thermal regulation than above-ground tanks [6], [91]. Thus, CAES is not likely to experience any significant storage capacity increase in the Arctic. This is reflected in the LCOS changes summarised below for three key scenarios.

The first scenario in Table 8 represents a high power cost and infrequent usage scenario. The second scenario has the same power cost and usage frequency as Scenario 1, but a longer discharge duration. The third scenario has the same discharge duration as Scenario 2, but a lower power cost and a 3X increase in cycles per year.

The first scenario has the highest LCOS and the lowest relative contribution of construction costs. This is because of its relatively high power cost and small plant scale, meaning the heating and charging costs are higher, while the construction costs are lower. Additionally, this is the scenario with the lowest amount of dispatched storage, which raises the LCOS. The RTE in this scenario is lowest because of the infrequent cycling and short discharge duration, which results in greater heat loss between cycles. Scenario 2 has a longer discharge duration which results in higher construction costs. Additionally, the power cost is still high and the charging periods are longer, which results in higher charging costs. It should be noted that just by increasing the plant's discharge duration, the LCOS decreased from a baseline of 2.13 USD/kWh to 0.86 USD/kWh. Scenario 3 has the lowest LCOS, mainly due to the frequent utilisation and low power cost. In this scenario, construction costs have by far the largest contribution to LCOS because the charging and heating costs are proportionally lower. Generally across all scenarios, locational construction costs dominate the LCOS change of Arctic CAES.

	Relative Contribution to LCOS Change (%)		
Cost Factor	Scenario 1	Scenario 2	Scenario 3
Construction Cost	84.96%	91.53%	93.89%
Heater/Insulation Cost	5.97%	2.61%	2.55%
EPC Cost	1.79%	0.78%	0.77%
Operational + Charging Costs (disc.)	7.28%	5.08%	2.79%
RTE at 20C	62.50%	63.70%	67.30%
RTE at -10C	62.03%	63.18%	66.92%
Temperate LCOS per kWh	$2.13	$0.86	$0.25
Arctic LCOS per kWh	$2.26	$0.92	$0.27
LCOS Change Due to Climate (%)	6.13%	7.24%	7.97%

Table 8: Contribution to LCOS Change in Arctic CAES Plants. Scenario 1: Power = 90 MW/10hr, Power Cost = 0.2 USD/kWh, CPY = 10. Scenario 2: Power = 90 MW/ 100hr, Power Cost = 0.2 USD/kWh, CPY = 10. Scenario 3: Power = 90 MW/100hr, Power Cost = 0.05 USD/kWh, CPY = 30.

12. Hydrogen Cost Modeling

This section aims to identify the key added costs associated with building a hydrogen ESS in the Arctic. For simplicity, it is assumed that hydrogen is created through LT-PEM electrolysis and converted back to power with a LT-PEM fuel cell. A fuel cell was chosen over a gas turbine configuration due to its lower air and noise pollution, its lack of moving parts, and its superior roundtrip efficiency. Proton Exchange Membrane was chosen over Alkaline or Solid Oxide technologies due to PEM's economies of scale, good power density, lower heating requirements, and relatively high efficiency. Although PEM electrolyzers and fuel cells are individually mature technologies, the integration of these systems for electricity storage in a PGP configuration is still nascent. Quantifying the costs of building and operating an Arctic PGP system is difficult because very few datapoints exist as of 2025, even in more temperate environments. This section aims to understand the key climate-related cost drivers associated with building and operating a PGP Plant in the Arctic. The cold-temperature effects listed below will be investigated to determine their net costs or savings.

- Increased power draw from heating systems
- Decreased power draw from cooling and compression systems
- Insulation for water tanks, feedlines, and PEM stack containers
- Winterisation of fluidic components, compressors, and dry coolers
- Locational factors such as labor, equipment rental, and materials cost
- Mass capacity gain of hydrogen tanks at cold temperatures

12.1. Hydrogen Operating Costs

This section aims to calculate the net change to PGP power demand in cold climates. A breakdown of the heating and cooling needs in a PGP plant is as follows. Generally, the products entering the electrolyzer or fuel cell require heating while the output products require cooling. Water entering an electrolyzer must be heated to match the stack temperature, to prevent thermal shock [92], [93]. Similarly, gas entering the fuel cell must be heated and humidified with a steam generator in order to ensure good conductivity through the proton exchange membrane [40]. Hydrogen exiting the electrolyzer must be cooled and dehumidified prior to storage, while hot water or steam exiting the fuel cell must be condensed and recirculated to the water storage tanks. Within the PEM stack itself, the membrane requires both heating during idle periods and cooling during operation. The membrane must be kept above freezing during idle periods to prevent ice formation, and preheated to 60-70℃ prior to startup [92], [93].

Designing a PEM-based system in the Arctic will naturally result in reduced cooling needs and increased heating loads, but it should also decrease the power required to compress the hydrogen and oxygen gases into their storage tanks at cold temperatures. This is dictated by the first law of thermodynamics and the perfect gas law, which together show that a lower temperature at the compressor inlet will result in a lower enthalpy change—and thus power— required to achieve the same pressure ratio and flowrate.

In order to quantify the net OPEX change, a series of first-order thermodynamic models were generated to represent the key heating and cooling processes in both the electrolyzer and fuel cell. The largest contributors to the OPEX change at a mean yearly temperature of -10℃ were shown to be 1). Increased

pre-heating required for the electrolyzer and fuel cell inlets, and 2). Reduced compressor power required to store hydrogen and oxygen gas at 300bar.

It can be assumed that any Arctic PGP Plant would be designed to utilise waste heat from its electrolysis and redox reactions, which is substantial due to the low process efficiency [93]. Even when assuming 25% heat exchanger losses, this waste heat is more than sufficient to cover all operational heating needs. Assuming waste heat utilisation is in place, the plant should see a net power *reduction* in most Arctic cases, mainly due to the reduction in oxygen and hydrogen compressor power during charging. It should be noted that this model assumes multi-stage compression with a nominal per-stage pressure ratio of 3:1, a compressor efficiency of 85%, and an inlet pressure of 30bar. The compression process was modeled using the same approach as CAES, but with CoolProps referencing equations of state for hydrogen versus air. The estimated power deltas, normalised by input power, for each thermodynamic process are shown in Figure 7.

Marker Number	OPEX Power Change Category	Change at -10C (%Total Power)	Change With Waste Heat Utilisation
1	Water Tank Heating	0.01%	0.01%
2	PEM Stack Water Pre-Heating	0.48%	-
3	Membrane Cooling during Operation	-0.04%	-
4	Membrane Heating during Idle	0.01%	0.001%
5	O_2 Compressor Power	-0.04%	-0.04%
6	H_2 Compressor Power	-0.18%	-0.18%
7	O_2 Gas Pre-Heating	0.40%	-
	Net Power Change	**0.63%**	**-0.21%**

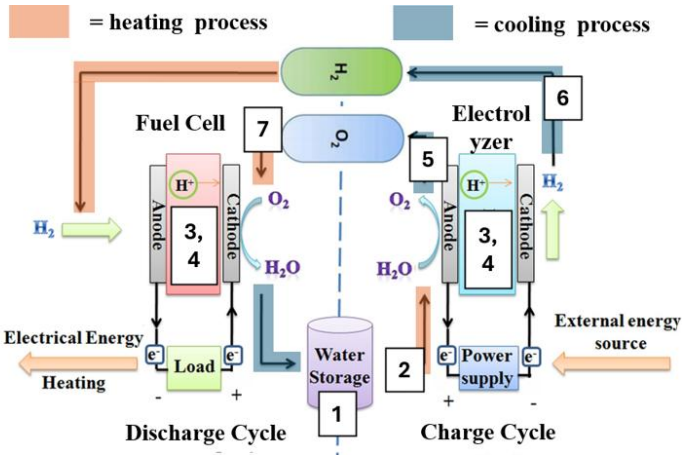

Figure 7: Power process flows within a Hydrogen PGP Plant

Membrane heating and cooling calculations follow the same methodology as the BESS thermal management system, since the two are very similar in design. Similar to BESS, the PEM stacks are generally containerised with a liquid coolant loop that runs through an air-cooled condenser to manage the waste heat. The key differences are the volumetric power density, operational range, and waste heat loads. PGP typically has a lower container volume than an equivalent BESS due to its inherent separation of energy and power— only the PEM stacks need be containerised and heated. PGP also has a much lower RTE than BESS and thus produces more waste heat, but also has a wider operational temperature range ($0°C<T_{stack}<80°C$) [40], [92], [93]. This allows for the use of dry coolers, which are generally less expensive than chillers on a per kW basis due to their lack of active refrigeration [94].

The methodology used to determine water tank heating power is outlined in the next section, as it is also pertinent to the CAPEX calculations. As seen in Figure 7, the overall change in operational costs in the Arctic is low when normalised by the large amount of power required for electrolysis. Lastly, it should be noted that this study does not consider the use of cryogenic LH_2 storage, but this option would also result in Arctic power savings, in the form of reduced refrigeration power.

12.2. Hydrogen Capital Costs

The impacts of cold climate on PGP CAPEX were determined with the aid of multiple cost models from sources such as the U.S. Department of Energy, Agora, and Electric Hydrogen [62], [67], [95]. A detailed cost breakdown was compiled for both electrolyzers and fuel cells and the most climate-sensitive categories were identified. The climate-driven CAPEX associated with water tank insulation and heating, compressor and dry cooler winterisation, and construction costs are detailed herein.

12.2.1. Water Tank Heaters & Insulation

For the water tank-related costs, the additional CAPEX was calculated by first estimating the number of water tanks and the tank dimensions required to achieve one full charge cycle at max power. An electrolyzer consumes approximately 15 kg of water for every 1 kg of hydrogen produced (including cooling processes), while a fuel cell produces approximately 8.5 kg of water for each kg of hydrogen consumed [96], [97]. Thus, the water usage is not entirely circular and new water entering the stack must first be deionised and purified. Every PGP plant will have provisions for on-site water processing and storage, and the total water storage volume is estimated using Equations 16 and 17 below [98].

$$(16) \quad H_2 Flowrate\ (kg/h) = \frac{P}{RTE \cdot C_e}$$

$$(17) \quad Water\ Storage\ Volume \simeq \frac{H_2 Flowrate \cdot CD \cdot WtoH}{\rho_{water}}$$

Where:

- *C_e = specific energy consumption of electrolyzer (approximately 55kWh/kg)*
- *WtoH = water to hydrogen mass ratio (approximately 15)*

The tank dimensions are then calculated assuming cylindrical tanks with a 1:1 height: diameter ratio and a capacity of up to two million litres per tank. A first-order thermodynamic model was created to quantify the costs associated with freeze prevention in the water system. Using the same heater cost assumption as the other ESS and a tank insulation thickness of 0.10 m, the total water heater cost was calculated by finding the heat input required to hold the tanks above the freezing point at a given outdoor reference temperature.

It should be noted that this model assumes good circulation and a uniform temperature gradient within the tanks. While this is an optimistic assumption, realistically the water system will be constantly recirculating regardless of climate, in order to maintain PEM water-quality standards [99]. A tank initialisation temperature of 10°C was assumed, given that waste heat would help to heat the bulk water tanks during operation. The tank water temperature is calculated over the average idle period in hourly increments at a range of ambient temperatures. Once the water temperature nears freezing, the tank heaters activate. The peak heater power is calculated using the maximum ΔT between the water and outdoors as well as the thermal resistance of the tank. The average heating power is then calculated using the same thermal resistance, but with the mean yearly temperature versus the wintertime low temperature. The heater energy, and indirectly the heating cost, is solved for by integrating heater power over the heater's yearly period of activation. The total insulation cost is solved for by multiplying the cost-per-unit-volume with the surface area and insulation thickness of each tank. The insulation cost of the feedlines is also accounted for in the model but has a very minor contribution to the overall costs.

12.2.2. Compressor Winterisation

Oxygen and Hydrogen gas, both products of electrolysis and feedstock for fuel cells, require compression into on-site storage tanks [100]. The compressors are generally located within an enclosure, so winterisation costs would involve insulation and heaters, similar to CAES. The enclosure volume was estimated from the power densities of other large-scale compressors [89], [90]. This metric is approximately 15 kW per square meter of floorspace. A ceiling height of 7 m was assumed, and the heat input required to maintain the compressor above -10℃ was accordingly solved for using the same methodology as with CAES. Generally, the heater and insulation costs for the water tanks, powertrain enclosure, and PEM stacks were found to be small in the context of the overall system costs, as summarised in Table 9.

12.2.3. Dry Cooler Winterisation

ITM, Plug, and Electric Hydrogen all cite -20℃ as the low temperature limit for operation for their PEM electrolyzers and fuel cells [96], [97], [101]. The dry coolers are generally the limiting factor and require customised features similar to the BESS chillers [99]. For the winterisation of dry coolers, the baseline costs were first estimated using a specific cost metric of 96 USD/kW [94]. Similarly, the valves, regulators, and other external fluidic components in the BoP infrastructure will need to be swapped for ruggedised cold-temperature versions. The cost of these fluidic components is estimated to be 1.5% of CAPEX according to a recent study on PEM manufacturing at scale [95]. A premium of +15% was added to the sticker prices of these components to cover the cost of customisation, similar to the chiller markup in the BESS section. Thus, the winterisation cost of the dry cooler system is estimated using Equation 18 below. This markup has a large uncertainty and will be further analyzed in the uncertainty analysis of section 13.1.

$$\Delta Cost_{cooler} \simeq \left(Load_{cooler} \cdot 96 \frac{USD}{kW} + CAPEX \cdot 0.015\right) \cdot ColdTemp\ Markup \tag{18}$$

$$Load_{cooler} = \frac{P}{RTE}(1 - RTE) \tag{19}$$

12.2.4. Construction Costs

Limited data is available on the construction cost of PGP plants, considering the nascent nature of this technology. Electrolyzers and fuel cells on the kW and low MW-scale are usually packaged alongside BoP infrastructure in a storage container. Nel Hydrogen makes modular, pre-fabricated 2.2 and 9 MW electrolyzers in standard 40ft storage containers, while Ballard Power Systems makes a more compact 200 kW PEM fuel cell for marine and stationary storage applications [102]. ITM Power's 20 MW "Poseidon" electrolyzer is also pre-fabricated and skid mounted [101]. As the ESS size grows, however, pre-fabrication becomes more difficult and locational costs associated with materials, labour, and equipment rentals in the Arctic could play a more significant role. The hydrogen storage system, whether above-ground or in caverns, will require significant on-site construction work as well. Industry tools such as LCOH+ and Agora do not differentiate construction costs from capital costs. A 2022 paper from Abdin et al. approximates construction costs as 10% of a hydrogen plant's CAPEX, which is how the specific construction cost in this model were derived [103]. The 25% locational markup was applied to the total construction cost in order to estimate the cost premium of building PGP in the Arctic. Uncertainty

associated with the onsite construction costs will be applied and reviewed in Section 13.1. The relative importance of these climate-related cost factors to LCOS are summarised in Table 9.

12.3. Net effect on the LCOS

Overall, the modest potential savings in operating costs do not offset the significant capital costs associated with winterising a PGP Plant. However, LCOS is determined not just by total cost, but also by the lifetime storage dispatched. If the capacity gain of the hydrogen tanks at cold temperature is actually utilised, an overall reduction in LCOS is possible in cold climates.

The thermodynamic relationship between density, temperature, and pressure of hydrogen gas was used to calculate the capacity gains across a wide temperature range as shown in Figure 8. Assuming a standard storage pressure of 300 bar, a tank at -20°C will be able to store approximately 16% more hydrogen than an identical tank in a 25°C climate.

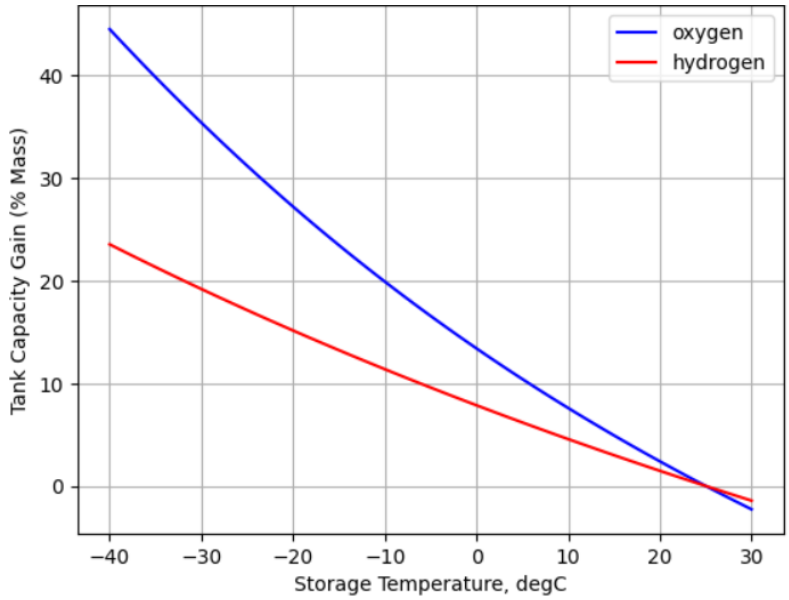

Figure 8: Mass capacity gain versus gas storage temperature at 300bar

It should be noted that this "extra" mass capacity will only lower the LCOS if actually utilised. For example, a community with access to low-cost electricity and multiple uses for H_2 gas is likely to take advantage of this extra storage capacity at cold temperatures. In contrast, if the available charging power for PGP is the bottleneck, the increased CAPEX will outweigh any gains in storage utilisation.

A variable was made to represent the amount of "extra" hydrogen capacity that actually gets used per charge cycle, called CF for "Capacity Factor." The CF is nominally assigned to be 75% in this study, but Table 9 demonstrates the effects of changing CF. In scenarios where CF>0, The extra storage capacity along with the extra charging costs are included in the calculation of the new LCOS. In Table 9 below, Scenario 1 represents a project with low utilisation, expensive power, and CF = 0. Scenario 2 is the same as Scenario 1 but with more frequent utilisation and a lower power cost. Scenario 3 is the same as Scenario 2 but with a capacity factor of 1.0.

	Relative Contribution to LCOS Change (%)		
Cost Factor	**Scenario 1**	**Scenario 2**	**Scenario 3**
Construction Cost	81.19%	82.30%	16.92%
Heater & Insulation Cost	3.01%	3.05%	0.63%
Custom Dry Cooler Cost	2.48%	2.52%	0.52%
Fluid Component Cost Increase	7.31%	7.41%	1.52%
EPC Cost Increase	3.84%	3.89%	0.80%
OPEX Change (disc.)	2.18%	0.84%	9.73%
Storage Capacity Increase (disc.)	0.00%	0.00%	69.88%
Temperate LCOS per kWh	$3.740	$1.195	$1.195
Arctic LCOS per kWh	$3.835	$1.226	$1.131
Total LCOS Change Due to Climate (%)	2.54%	2.59%	-5.36%

Table 9: Contribution to LCOS Change in Arctic PGP Plants. Scenario 1: 10 MW/1000hrs, powercost = 0.20 USD/kWh, CPY = 1, CF = 0.0. Scenario 2: 10 MW/1000hrs, powercost = 0.05 USD/kWh, CPY = 3, CF = 0.0. Scenario 3: 10 MW/1000hrs, powercost = 0.05 USD/kWh, CPY = 3, CF = 1.0

As seen in Table 9, construction costs dominate the first two scenarios and storage capacity increase dominates scenario 3, assuming a mean yearly temperature of -10°C. Scenario 3 is the only scenario of this study to show a *decrease* in LCOS under Arctic conditions, due to the exploitation of improved hydrogen density at cold temperatures. Scenario 1 has by far the most expensive LCOS, considering the infrequent usage of the system and the expensive power cost of 0.20 USD/kWh.

The LCOS of hydrogen PGP is more sensitive to charging cost than any other storage technology in this study, due to its low RTE. Thus, a plant with access to cheap renewable power will have a much lower LCOS than a plant which uses grid power at a high utility rate. The effect of Arctic climate on hydrogen's LCOS depends heavily on the utilisation assumptions. If the extra storage capacity at cold temperatures is actually utilised, which is likely in communities that have multiple use cases for hydrogen beyond electricity storage, PGP plants could become a more attractive option for long duration storage in the Arctic.

13. Results Discussion

As stated in the methodology section, this study involves the creation of a master script which calls each individual storage model with the common inputs of power, discharge duration, charges per year, discount rate, project lifespan, power cost, and reference temperatures. The results of each individual model from Sections 8 through 12 are aggregated across a range of discharge durations and frequencies to create a competitive landscape plot similar to Schmidt and Staffel's Figure 3. The left subplot in Figure 9 below shows the storage technology with the lowest LCOS for any combination of discharge duration and CPY. This plot was created using the specific cost data from Table 3 and the LCOS equations from the methodology section. The right subplot shows the new competitive landscape when climate factors are taken into consideration. The operating points that have switched technology preference are highlighted for clarity. It should be noted that both axes are plotted on a log scale and the diagonal denotes where the combination of discharge duration and charging frequency exceeds the total hours in a year. Both plots

assume a fixed power of 100 MW, a project lifespan of 50 years, a discount rate of 8%, and a power cost of 0.05 USD/kWh.

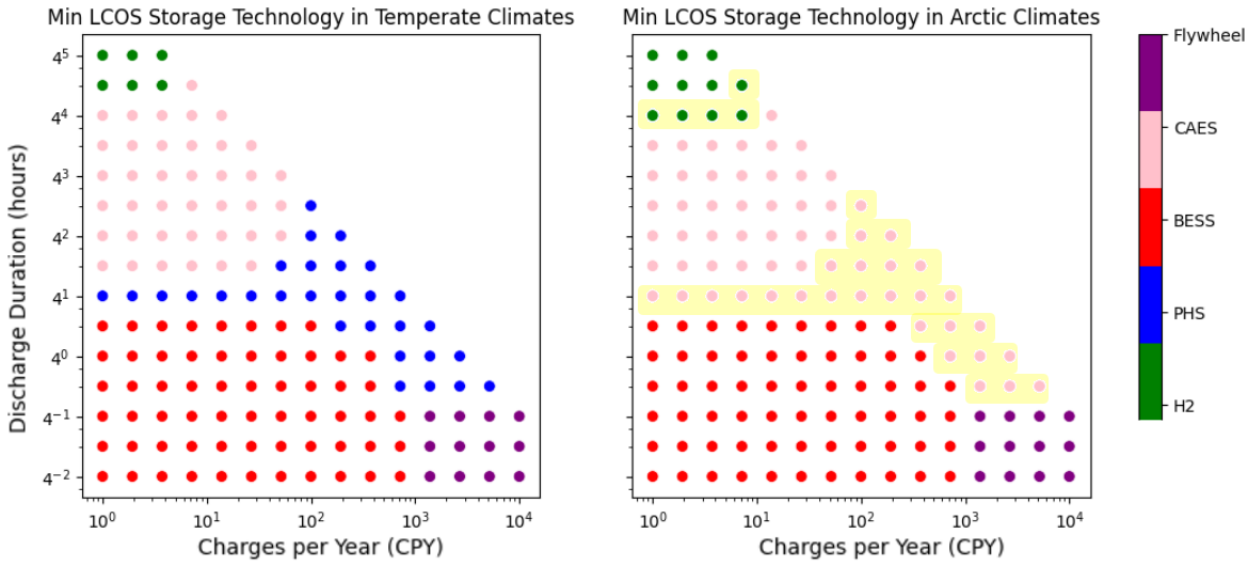

Figure 9: Competitive landscape of ESS at baseline (left) and Arctic (right) conditions. P= 100 MW, project lifespan = 50 years, r = 8% and power cost = 0.05 USD/kWh.

A key takeaway from Figure 9 is that the competitiveness of energy storage technologies like PHS and hydrogen are more affected by climate than power storage technologies like Flywheels and BESS. For Arctic PHS, the high construction costs and the capacity loss due to reservoir freezing increases its LCOS to the point where it's no longer competitive at this power level. For hydrogen, the LCOS is highly dependent on the utilisation of extra storage capacity that becomes available at low temperatures. This plot assumes that 75% of the "extra" storage capacity caused by the density change of H_2 at a mean yearly temperature of -10°C is used. Under these conditions, hydrogen ESS could become cost competitive for applications with discharge durations as low as 175 hours, as compared to approximately 300 hours in temperate locations. Adiabatic CAES experiences heightened construction costs in the Arctic, as well as higher charging costs associated with a slightly lower RTE in colder climates. Conversely, the BESS and flywheel technologies show a slight increase in LCOS but still dominate the same operating ranges due to their lower construction costs, high power-density, and efficient thermal management systems.

Building on this data, Figure 10 below shows the minimum Arctic LCOS gradient on the lefthand plot. The righthand plot shows the LCOS change as a percentage of the baseline LCOS for the competitive technology in each scenario. Apart from hydrogen, all other storage applications become more expensive in the Arctic, though the projects with highest utilisation tend to have the smallest LCOS change. This is because the upfront costs of building ESS in the Arctic generally get diluted as the lifetime OPEX and the cumulative dispatched storage grow.

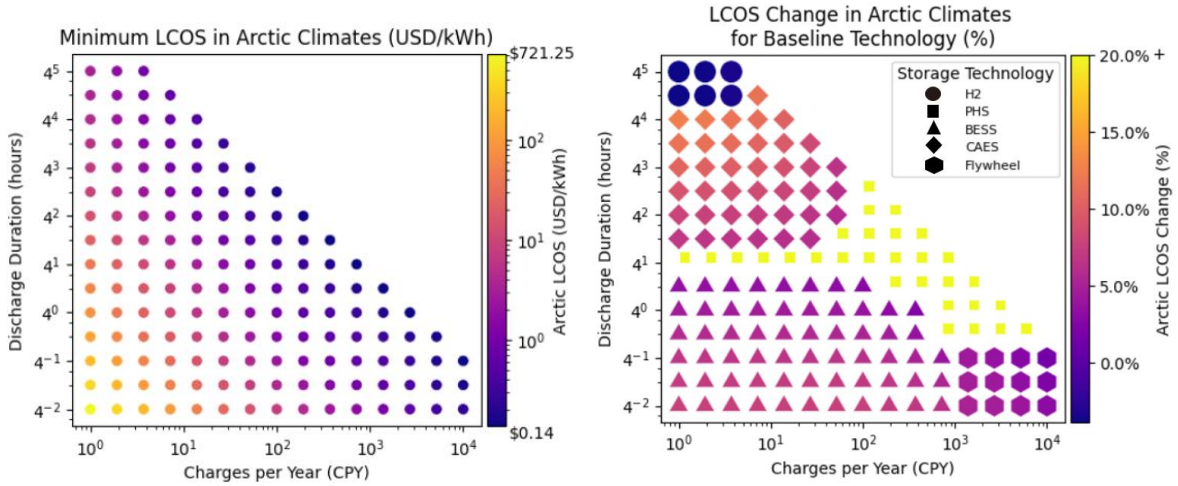

Figure 10: Minimum LCOS gradient (left) and LCOS change of baseline technology (right) in Arctic conditions

The LCOS changes from the righthand plot above were averaged by technology, only considering the datapoints where each technology was competitive in the baseline case. The resulting average LCOS change across each storage type is summarised in the bar chart in Figure 11. This is a reasonable illustration of the climate sensitivity across all storage technologies. Note that these values are highly sensitive to input assumptions such as power capacity and power cost, which will be explored further in the following sections. Figure 11 shows that, in this scenario, the technology with the highest economic sensitivity to Arctic climate is PHS, followed by CAES, BESS, flywheel, and hydrogen.

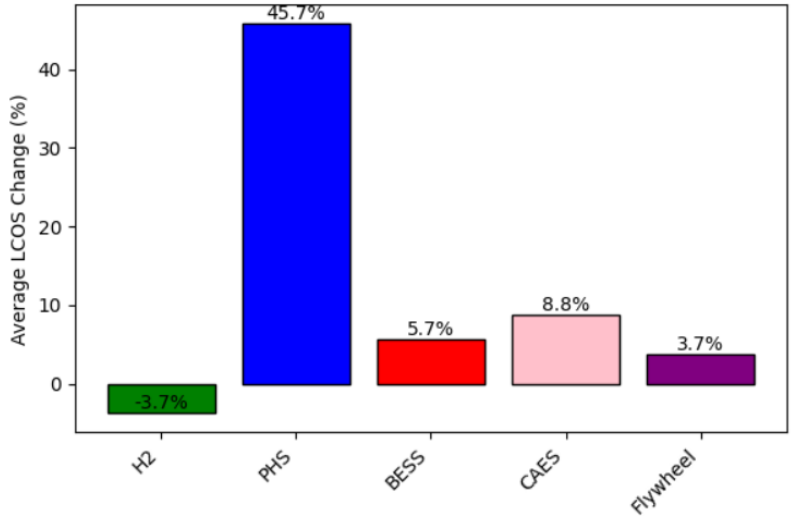

Figure 11: Average LCOS change in the Arctic by technology. P = 100 MW, Power Cost = 0.05 USD/kWh, r = 8%, CF = 0.75

It should be noted that there are many sources of uncertainty in these summary plots. There are many factors beyond climate that will affect LCOS, including regional variations in labor costs, building codes, geography, existing infrastructure, and taxes. Some key uncertainties will be identified in the following section, along with their effects on levelised storage costs.

13.1. Uncertainty Analysis

In this study, the baseline LCOS will be considered as fixed and uncertainties will only be applied to climate-related variables in order to determine the range of possible LCOS changes in the Arctic. Uncertainties have been applied to all of the key Arctic-specific variables shown in Table 10. The master script applies the nominal, best-case, and worst-case combinations of these uncertainties from Table 10 to calculate the range of possible LCOS changes for individual projects.

Storage Type	Parameter	Nominal Value	Unit	Lower Limit	Upper Limit
Common Params	Heat Exchanger Effectiveness	0.75		-20%	20%
	Heater Cost	0.5	USD/W	-20%	20%
	Insulation Cost	600	USD/m3	-40%	40%
	Cold-rated Component Markup	15	%	-50%	50%
	Construction Time	See Table 3	years	0%	50%
	Locational Markup on Construction	25	%	-50%	50%
BESS	Specific Chiller Cost	130	USD/kW	-50%	50%
Hydrogen	Capacity Factor (CF)	0.75		-100%	33%
	FEED cost	30	% CAPEX	-20%	20%
CAES	Compressor Rating	-10	C	-100%	100%
	Specific Capacity Cost Factor (TES)	1		-25%	25%
	Thermal Energy Density Factor	1		-25%	25%
PHS	Underground Powerstation Fixed Cost	$67,000,000	USD	-70%	70%
	Snow depth	0.5	m	-50%	50%
	Reservoir Aspect Ratio	50		-50%	50%
Flywheel	Specific Chiller Cost	130	USD/kW	-40%	40%

Table 10: Key uncertainties applied to Arctic LCOS calculation

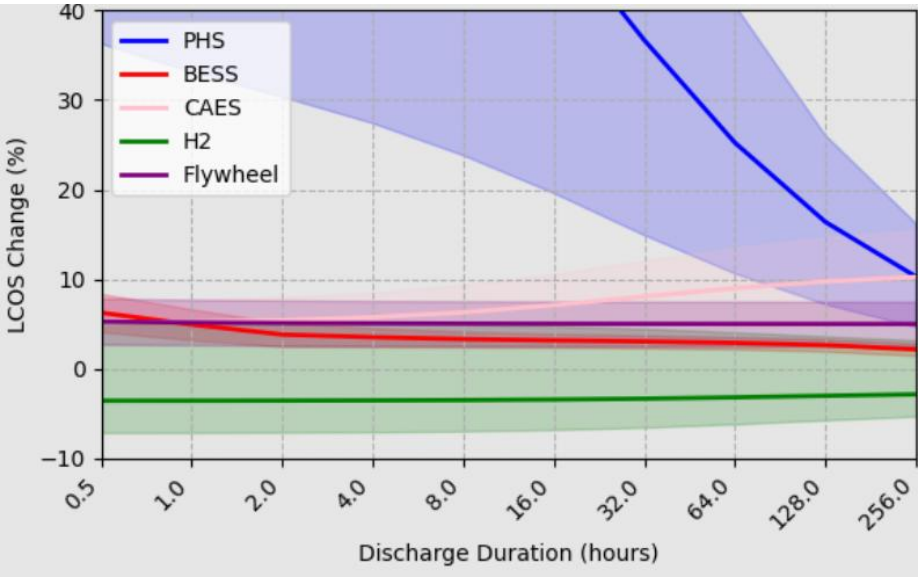

Figure 12: LCOS change from baseline to Arctic conditions for storage technologies at incremental discharge durations. P=100 MW, CPY = 30, r = 8%, project lifespan =50years

The results from Table 10 were used to create Figure 12 above for a sample case of P = 100 MW, Power cost = 0.05 USD/kWh, CPY = 30, Discount rate = 8% and project lifespan = 50years. Each line represents the nominal LCOS change from baseline to Arctic conditions, with the shaded regions indicating the bounds of uncertainty.

Pumped hydro has the largest LCOS change and error band, though uncertainty decreases as discharge duration increases. This is because the uncertainties affecting capacity loss and fixed capital cost become less significant as the yearly OPEX and storage dispatch increase. Hydrogen has the next largest error band, due to the large uncertainty assigned to capacity factor. Recall that the capacity factor, which ranges from 0 to 1, represents the portion of additional storage capacity—arising from hydrogen's higher energy density in the Arctic—that is actually utilised.

As seen in Figure 12, the LCOS change of CAES *increases* with discharge duration, unlike the other storage technologies. Recall that CAES charging cost increases due to its lower RTE at colder temperatures, as explained in Section 11.1. Thus, the climate effect on CAES becomes more pronounced at longer discharge durations. BESS and Flywheels both have fairly low uncertainty regions, but the LCOS of BESS decreases more sharply with discharge duration than FESS. This is because for BESS, heating costs decrease as discharge duration increases, as there is less idle time between charges. Flywheel maintains a relatively constant LCOS change, but the LCOS value itself becomes prohibitively high over durations of approximately one hour.

Generally, the magnitude of uncertainty for each technology correlates with the magnitude of on-site construction required, indicating that the LCOS results are most sensitive to the locational markup factor. Hydrogen's capacity factor is very influential to its own LCOS as well. The uncertainties affecting TMS cost calculations are found to be less significant in comparison, as evidenced by BESS' relatively narrow uncertainty range despite its having the highest proportion of TMS-related costs. In addition to the climate-related uncertainties from Table 10, the competitive landscape shown in Figure 9 will also be affected by

power level, regional power cost, discount rate, and maintenance factors. These sensitivities will be explored in the following sections.

13.2. Power Level Sensitivity

Modifying the plant scale in terms of peak power capacity can have varying effects on LCOS and competitiveness. A technology with high fixed costs on top of the specific capital costs, such as PHS, will become more cost-competitive at larger scales where the fixed costs become less significant. This can be seen in Figure 13, where the high upfront costs of building an underground power station for an Arctic PHS plant become less significant at the 1 GW scale (right). For modular technologies with low fixed costs, the LCOS can be surprisingly insensitive to power level, as the ratio between marginal costs and marginal storage capacity remains fairly constant at scale.

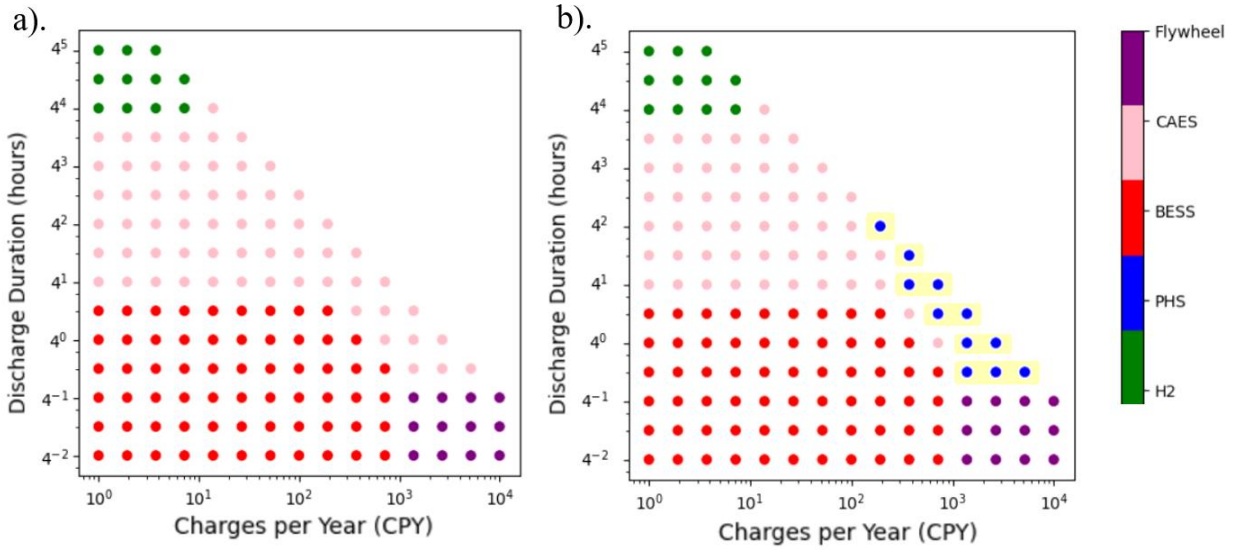

Figure 13: Competitive Arctic ESS landscape for various power levels a). P = 10 MW and b). P = 1000 MW, r =8%, Power Cost = 0.05 USD/kWh, Project Lifespan =50 years

13.3. Power Cost Sensitivity

Generally, a region with high power costs will favor storage technologies with a high RTE. As seen in Figure 14, increasing the regional power cost from 0.05 to 0.20 USD/kWh causes the technology with the lowest RTE —hydrogen— to lose competitiveness. PHS may even be a better option than CAES in certain scenarios due to its lower charging cost, though this is countered somewhat by its higher heating costs. Interestingly, BESS loses some ground to CAES at the higher utilisation data points even though it has a superior RTE. This is due to its higher TMS power consumption and its reduced storage capacity at high cycle counts. Overall, the power cost has a significant effect on LCOS as seen in Figure 14, primarily due to higher charging and heating costs. The minimum LCOS for any storage application rises from 0.14 USD/kWh to 0.35 USD/kWh when the power cost increases from 0.05 to 0.20 USD/kWh. Thus, the regional access to low-cost power, often in the form of renewable energy, will be an important decision-making factor for Arctic ESS development.

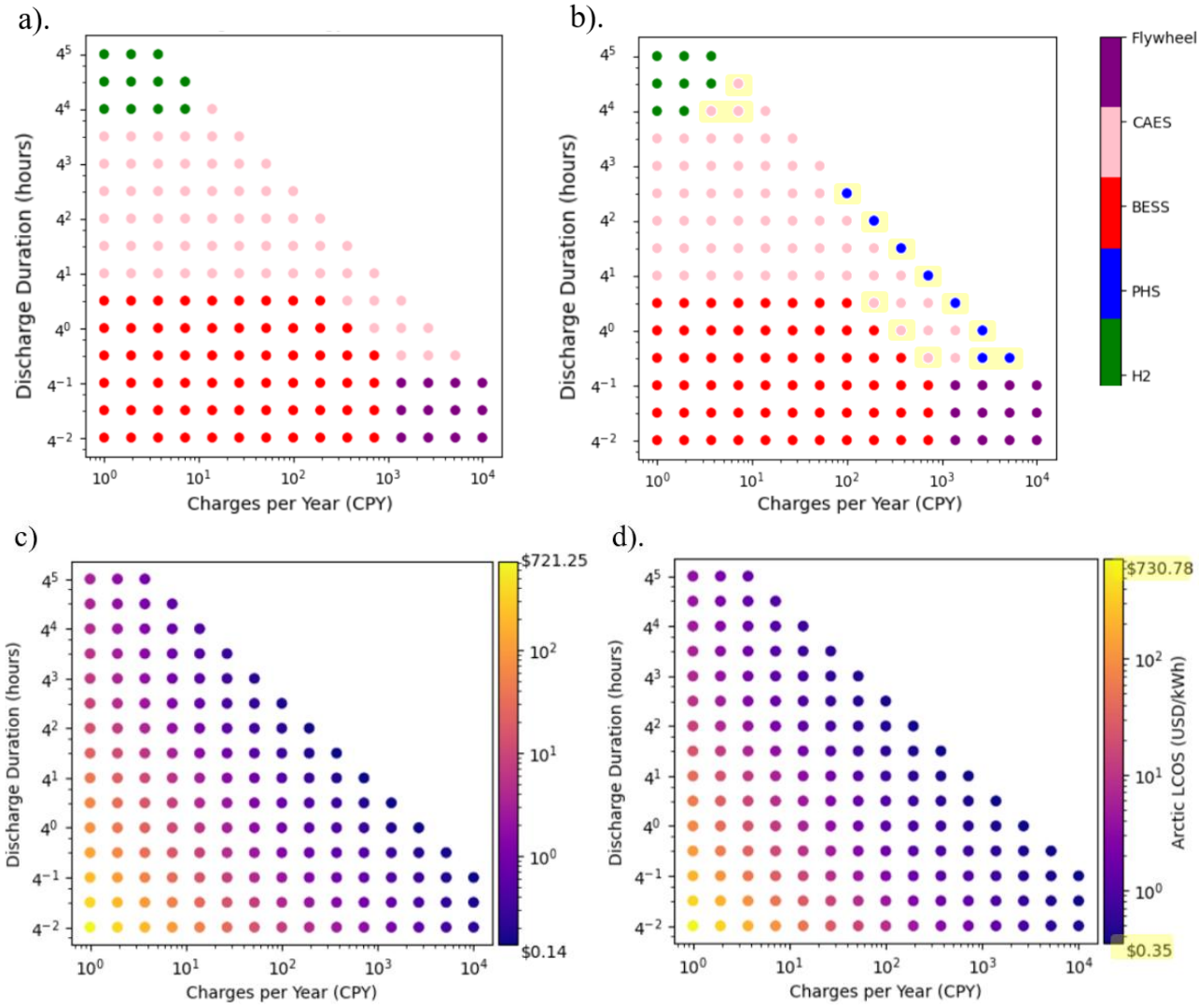

Figure 14: Competitive landscapes of Arctic ESS at varying power costs. a). power cost = 0.05 USD/kWh, b). power cost = 0.20 USD/kWh. Min LCOS gradients at c). power cost = 0.05 USD/kWh d). power cost = 0.20 USD/kWh. P = 100 MW, r = 8%

13.4. Discount Rate Sensitivity

A storage project with a high discount rate implies that future costs and storage dispatch are discounted more, so the upfront CAPEX plays an even more significant role in the LCOS determination. This tends to favor technologies with lower upfront costs and shorter lifespans, since short-term profits are prioritised over long-term profits, which are highly discounted. Conversely, a state-funded project with a low discount rate prioritises long-term profits and upfront costs become less significant. Thus, Figure 15 shows how lowering the discount rate from 8% (right) to 2% (left) enables PHS to become somewhat more competitive with CAES, even in the Arctic. CAES, in turn, becomes more competitive at longer discharges because its discounted charging costs are significantly lower than hydrogen's. Similarly, flywheels can become competitive with BESS across a wider range of cycle frequencies despite their higher upfront costs. As with

the other plots, the highlighted datapoints denote where the results have changed from the "baseline case". This illustrates the importance of considering discount rates when developing an Arctic ESS.

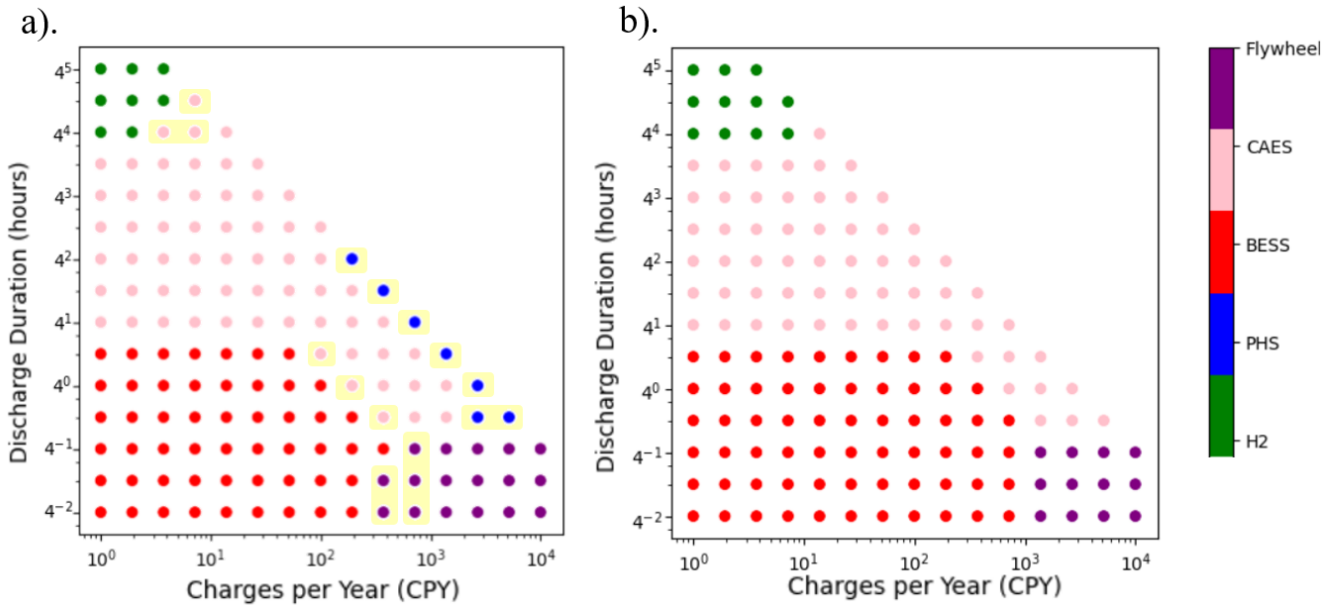

Figure 15: Competitive landscapes of Arctic ESS at various discount rates. a). r = 2% b). r = 8%

13.5. Maintenance Cost Sensitivity

Arctic ESS can incur heightened maintenance costs due to the extreme environment and the lack of on-site repair capabilities. An NREL study on Arctic Renewable Energy stresses the importance of thoroughly testing subassemblies in representative conditions prior to shipping [1]. This is where modular technologies like BESS, flywheels, and hydrogen PGP have an advantage. These self-contained products are easier to test at their point of origin. There is very little data available on the effect of Arctic climate on plant maintenance costs, so a sensitivity study was conducted to determine the impact of increased maintenance costs.

In this study, O&M costs were first doubled and the effect on LCOS and competitiveness was found to be negligible. Next, maintenance costs were multiplied by a factor of five and finally there was a discernible cost change for applications with low storage throughput, as seen in Figure 16. The highlighted datapoints represent operating conditions where the competitive technology has flipped, as compared to the baseline case in Figure 9. Technologies with lower maintenance costs like BESS and flywheels were favored while higher-maintenance technologies like Hydrogen lose competitiveness [6]. Generally, however, the LCOS and competitiveness of ESS are less sensitive to O&M cost factors, provided they don't result in prolonged plant shutdowns.

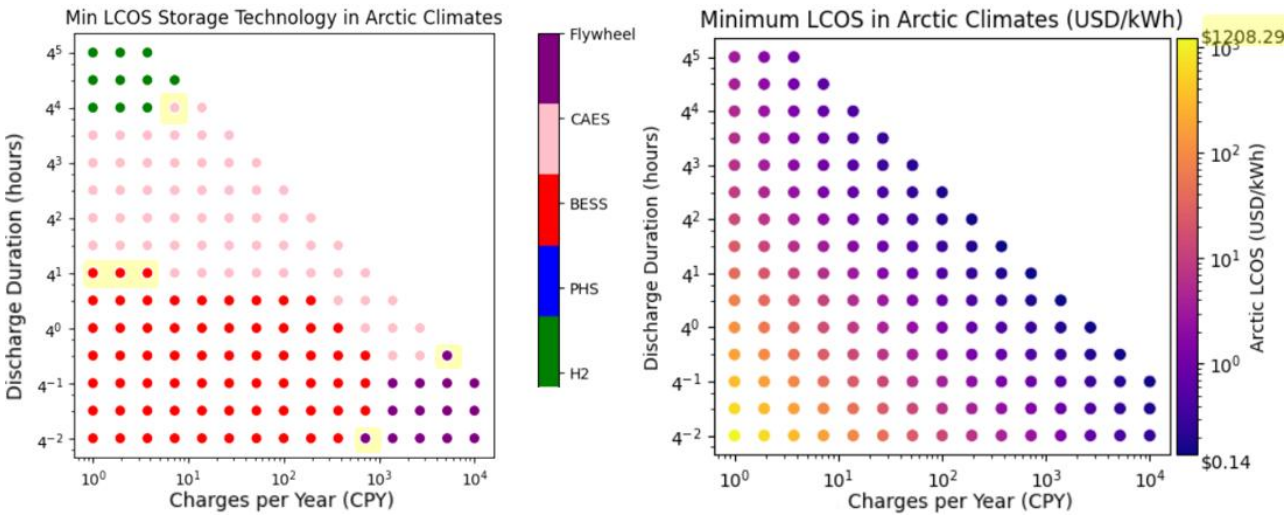

Figure 16: Competitive landscape and min LCOS values for Arctic ESS: maintenance costs increase by 5X

13.6. Future Applicability

This storage modelling tool is highly parameterised for forward compatibility. As technological innovation and economies of scale progress, the competitive landscape will naturally shift. Figure 17 shows a future scenario in which hydrogen and BESS have improved performance, based on industry trends such as the experience curves from Figure 2. In this scenario, lithium-ion BESS is assumed to have an RTE of 92% and a cycle life of 7,000, while hydrogen's specific investment cost has decreased by 20% and its RTE has increased to 48%. Unsurprisingly, this results in an increased range of applications where BESS and hydrogen PGP are competitive. The model predicts that, assuming a power cost of 0.05 USD/kWh, hydrogen PGP could become competitive at discharge durations of 128 hours. Similarly, BESS becomes competitive up to cycle frequencies of approximately 2,100 CPY. These two technologies were chosen as an example for their rapid development in recent years, but similar developments in other storage technologies are also possible.

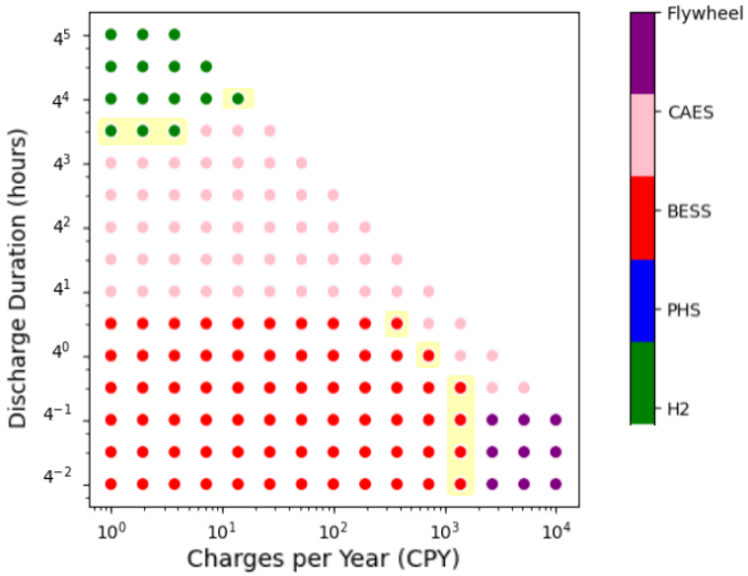

Figure 17: Competitive Landscape of Arctic ESS in a future scenario where BESS RTE = 92% and cycle life = 7,000. Hydrogen RTE = 48% and Specific Investment cost = 4,000 USD/kW.

14. Conclusion

A preliminary literature review draws a clear correlation between high renewable penetration and low electricity tariffs in remote energy systems across the Arctic. As many of the case studies from this review have shown, the addition of energy storage to variable renewable energy systems is crucial for increased resilience and reduced diesel usage. Currently, the limited amount of stationary storage in the Arctic is mainly in the form of BESS, but there may be potential for more diversified solutions such as flywheels, pumped hydropower, compressed air, thermal, and hydrogen PGP storage. However, the best technology choice is highly project-specific.

This study developed and applied a technoeconomic framework to evaluate the competitiveness of multiple energy storage technologies under Arctic conditions. The methodology integrated climate-specific factors into baseline cost models to assess their effect on the Levelised Cost of Storage (LCOS). The analysis combined literature-based technoeconomic parameters with adjustments for Arctic-specific operating expenses, capital markups, and lifetime storage capacity changes. This approach enabled a side-by-side comparison of storage technologies under a range of discharge durations and cycle frequencies, while also accounting for key uncertainties.

The results of this study indicate that, unsurprisingly, Arctic LCOS increases as compared with the temperate baseline in most scenarios. The only potential exception to this is hydrogen PGP, which can see reduced LCOS in applications which allow for the full utilisation of hydrogen's higher density and lower compression power in Arctic climates. The demand for hydrogen PGP is still limited, however, due to its capital-intensive nature and commercial immaturity.

Generally, energy storage applications are shown to be more sensitive to Arctic climatic factors than power storage applications. The large amount of on-site construction, particularly in PHS and CAES, plays a key role in this distinction. PHS is the most negatively affected, with large cost impacts associated with building an underground power station, ice-related capacity loss, and blockage prevention in the form of trash rack heaters. CAES also displays significant economic sensitivity to climatic factors, partially due to its high locational construction costs, and partially because its RTE decreases slightly with ambient temperature. BESS requires advanced thermal management to prevent climate-induced degradation. BESS climate-related costs are less driven by on-site construction costs than other ESS (though it is still a major factor) and operational costs play a more significant role. The net change in OPEX is highly sensitive to the idle-to-operational ratio, since Arctic BESS will see higher heating costs during idle periods and lower cooling costs during operational periods. Flywheels are least affected by climate due to their wide operational temperature range and modular nature.

The precise range of discharge durations and cycle frequencies over which an ESS is cost competitive depends on many factors such as power level, regional power cost, and discount rate. Power level can have a large effect on LCOS in scenarios with high fixed costs, where a low power output becomes uneconomical. Regional power prices also strongly influence technology choice, with high utility rates favoring high-RTE systems. Higher discount rates shift the balance from long-lived, capital-intensive options towards lower-cost, shorter-lived ones. Maintenance cost was shown to play a relatively minor role, provided the maintenance does not incur a prolonged shutdown.

Climate-specific uncertainties around key variables were applied to assess the possible range of levelised costs for each technology. Sixteen variables were included in this uncertainty analysis, such as heat exchanger effectiveness, heater cost, insulation cost, and construction time. It was found that Arctic LCOS was generally more sensitive to variables affecting the locational construction costs than those concerning the thermal management costs.

In summary, BESS in the Arctic is still competitive across most short to mid-duration applications, but even more so when discount rates and locational construction costs are high. Flywheels are most competitive in Arctic applications with high cycle frequencies and low discount rates. While generally not very competitive in the Arctic, PHS can make sense in niche applications with pre-existing dam infrastructure and flood management needs. However, PHS is found to be more competitive in the Arctic at larger scales, with low discount rates and higher utilisation. Arctic A-CAES is most competitive in regions with suitable underground caverns and nearby waste heat sources to augment the thermal energy storage. Lastly, Arctic PGP is most competitive in areas with low power costs, high VRE penetration, and multiple uses for hydrogen.

While Arctic conditions introduce non-negligible cost challenges, energy storage remains a viable strategy for reducing diesel dependence and enhancing resilience. Arctic plants with high utilisation will generally have a lower LCOS penalty, as most climate-related expenses are upfront costs and will be diluted with greater utilisation. Achieving meaningful fossil fuel displacement will require deeper integration of ESS into Arctic grids, and the insights from this study provide a foundation for anticipating both the hidden costs and potential benefits of such developments.

References

[1] B. Anderson, R. Jordan, and I. Baring-Gould, “Distributed Renewables for Arctic Energy: A Case Study,” NREL/TP-5000-84391, 1922401, MainId:85164, Jan. 2023. doi: 10.2172/1922401.

[2] D. Chade, T. Miklis, and D. Dvorak, “Feasibility study of wind-to-hydrogen system for Arctic remote locations – Grimsey island case study,” *Renewable Energy*, vol. 76, pp. 204–211, Apr. 2015, doi: 10.1016/j.renene.2014.11.023.

[3] M. Temiz and I. Dincer, “A unique ocean and solar based multigenerational system with hydrogen production and thermal energy storage for Arctic communities,” *Energy*, vol. 239, p. 122126, Jan. 2022, doi: 10.1016/j.energy.2021.122126.

[4] H. Toal, C. Pike, D. Riley, and L. Burnham, “Optimizing a Hybrid East-West Vertical and Equator-Facing Bifacial Solar PV Array for a High-Latitude Microgrid,” in *2024 IEEE 52nd Photovoltaic Specialist Conference (PVSC)*, Seattle, WA, USA: IEEE, Jun. 2024, pp. 1775–1777. doi: 10.1109/PVSC57443.2024.10749065.

[5] “Energy Storage: 10 Things to Watch in 2024,” BloombergNEF. Accessed: Apr. 08, 2025. [Online]. Available: https://about.bnef.com/blog/energy-storage-10-things-to-watch-in-2024/

[6] O. Schmidt and I. Staffell, *Monetizing Energy Storage: a toolkit to assess future cost and value*. Oxford University Press, 2023.

[7] X. Han *et al.*, “Comparative life cycle greenhouse gas emissions assessment of battery energy storage technologies for grid applications,” *Journal of Cleaner Production*, vol. 392, p. 136251, Mar. 2023, doi: 10.1016/j.jclepro.2023.136251.

[8] D. Javeline *et al.*, “Russia in a changing climate,” *WIREs Climate Change*, vol. 15, no. 2, p. e872, Mar. 2024, doi: 10.1002/wcc.872.

[9] D. Yumashev *et al.*, “Climate policy implications of nonlinear decline of Arctic land permafrost and other cryosphere elements,” *Nat Commun*, vol. 10, no. 1, p. 1900, Apr. 2019, doi: 10.1038/s41467-019-09863-x.

[10] T. Heleniak, “The future of the Arctic populations,” *Polar Geography*, vol. 44, no. 2, pp. 136–152, Apr. 2021, doi: 10.1080/1088937X.2019.1707316.

[11] J. Wertheim, “60 Minutes - Newsmakers Why Trump wants Greenland, and what people who call the world’s largest island home have to say about it,” *CBS News*, Apr. 13, 2025. Accessed: Apr. 15, 2025. [Online]. Available: https://www.cbsnews.com/news/why-trump-wants-greenland-60-minutes-transcript/

[12] K. Pechko, “Rising Tensions and Shifting Strategies: The Evolving Dynamics of US Grand Strategy in the Arctic,” *The Arctic Institute*, Jan. 07, 2025. Accessed: Apr. 15, 2025. [Online]. Available: https://www.thearcticinstitute.org/rising-tensions-shifting-strategies-evolving-dynamics-us-grand-strategy-arctic/

[13] A. Kolker, R. Garber-Slaght, B. Anderson, T. Reber, K. Zyatitsky, and H. Pauling, “Geothermal Energy and Resilience in Arctic Countries,” NREL/TP-5700-80928, 1862005, MainId:78706, Apr. 2022. doi: 10.2172/1862005.

[14] “Annual Report 2023.” Nukissiorfiit, 2023. Accessed: Apr. 15, 2025. [Online]. Available: https://nukissiorfiit.gl/media/4d90c4ca-ed2b-4057-be2f-20c919dbc1bc/9KS7aw/%C3%85rsregnskaber/%C3%85rsrapport%202023%20-%20Engelsk%20-%2002.pdf

[15] E. S. Amundsen and L. Bergman, “Why has the Nordic electricity market worked so well?,” *Utilities Policy*, vol. 14, no. 3, pp. 148–157, Sep. 2006, doi: 10.1016/j.jup.2006.01.001.

[16] O. V. Zhdaneev, V. A. Karasevich, A. V. Moskvin, and R. R. Khakimov, “Application of renewable and hydrogen energy in the Arctic by the example of modernizing the energy system of the Arctic settlement of Khatanga,” *International Journal of Hydrogen Energy*, vol. 95, pp. 267–277, Dec. 2024, doi: 10.1016/j.ijhydene.2024.11.183.

[17] CEIC, "Electricity Consumption: FE: Republic of Sakha (Yakutia)." Accessed: Apr. 15, 2025. [Online]. Available: https://www.ceicdata.com/en/russia/electricity-consumption-by-region/electricity-consumption-fe-republic-of-sakha-yakutia
[18] T. Gavrilyeva, "Energy consumption and CO2 emissions in the northern cities (case of Yakutia)," Yakut Centre of Siberian Branch of Russian Academy of Sciences, 2014. Accessed: Apr. 15, 2024. [Online]. Available: https://www-sre.wu.ac.at/ersa/ersaconfs/ersa16/Paper1002_TuyaraGavrilyeva.pdf
[19] N. S. Volotkovskaya, N. N. Kugusheva, A. S. Semenov, I. A. Yakushev, S. N. Pavlova, and O. V. Kolosova, "Structure, condition, and prospects of electrical grids in the Republic of Sakha (Yakutia)," *E3S Web Conf.*, vol. 124, p. 04001, 2019, doi: 10.1051/e3sconf/201912404001.
[20] A. Fly, I. Kirkpatrick, and R. Chen, "Low temperature performance evaluation of electrochemical energy storage technologies," *Applied Thermal Engineering*, vol. 189, p. 116750, May 2021, doi: 10.1016/j.applthermaleng.2021.116750.
[21] D. Wolf and M. Budt, "LTA-CAES – A low-temperature approach to Adiabatic Compressed Air Energy Storage," *Applied Energy*, vol. 125, pp. 158–164, Jul. 2014, doi: 10.1016/j.apenergy.2014.03.013.
[22] A. Tomczewski, "Operation of a Wind Turbine-Flywheel Energy Storage System under Conditions of Stochastic Change of Wind Energy," *The Scientific World Journal*, vol. 2014, pp. 1–16, 2014, doi: 10.1155/2014/643769.
[23] A. Benato and A. Stoppato, "Pumped Thermal Electricity Storage: A technology overview," *Thermal Science and Engineering Progress*, vol. 6, pp. 301–315, Jun. 2018, doi: 10.1016/j.tsep.2018.01.017.
[24] A. Colthorpe, "Tesla Megapack on fire in 'minor incident' at battery storage site in Australia," *Energy Storage News*, Sep. 27, 2023. Accessed: Apr. 14, 2025. [Online]. Available: https://www.energy-storage.news/tesla-megapack-on-fire-in-minor-incident-at-battery-storage-site-in-australia/
[25] B. R. David, S. Spencer, J. Miller, S. Almahmoud, and H. Jouhara, "Comparative environmental life cycle assessment of conventional energy storage system and innovative thermal energy storage system," *International Journal of Thermofluids*, vol. 12, p. 100116, Nov. 2021, doi: 10.1016/j.ijft.2021.100116.
[26] C. Murray, "Moss Landing 'is not a market-moving event' for BESS insurance," *Energy Storage News*, Mar. 10, 2025. Accessed: Apr. 14, 2025. [Online]. Available: https://www.energy-storage.news/moss-landing-is-not-a-market-moving-event-for-bess-insurance/
[27] B. E. Worku, S. Zheng, and B. Wang, "Review of low-temperature lithium-ion battery progress: New battery system design imperative," *Intl J of Energy Research*, vol. 46, no. 11, pp. 14609–14626, Sep. 2022, doi: 10.1002/er.8194.
[28] Z. Bai *et al.*, "Low-Temperature Sodium-Ion Batteries: Challenges and Progress," *Advanced Energy Materials*, vol. 14, no. 17, p. 2303788, May 2024, doi: 10.1002/aenm.202303788.
[29] "Amber Kinetics M32 Datasheet," Amber Kinetics. Accessed: Aug. 21, 2025. [Online]. Available: https://www.amberkinetics.com/wp-content/uploads/2020/05/Amber-Kinetics-DataSheet.pdf
[30] E. Beinhocker and J. D. Farmer, "The Clean Energy Revolution Is Unstoppable," *The Wall Street Journal*, Feb. 28, 2025. Accessed: Apr. 14, 2025. [Online]. Available: https://www.wsj.com/business/energy-oil/thecleanenergyrevolution-is-unstoppable-88af7ed5
[31] "Hydropower expansion and improved management in response to increased glacier melt in Iceland," Climate ADAPT. Accessed: Aug. 19, 2025. [Online]. Available: https://climate-adapt.eea.europa.eu/en/metadata/case-studies/hydropower-expansion-and-improved-management-in-response-to-increased-glacier-melt-in-iceland
[32] Hydrostor Inc., "Advanced Compressed Air Energy Storage." Accessed: Aug. 19, 2025. [Online]. Available: https://hydrostor.ca/technology/
[33] A. Aghahosseini and C. Breyer, "Assessment of geological resource potential for compressed air energy storage in global electricity supply," *Energy Conversion and Management*, vol. 169, pp. 161–173, Aug. 2018, doi: 10.1016/j.enconman.2018.05.058.

[34] T. Yang, W. Liu, G. J. Kramer, and Q. Sun, "Seasonal thermal energy storage: A techno-economic literature review," *Renewable and Sustainable Energy Reviews*, vol. 139, p. 110732, Apr. 2021, doi: 10.1016/j.rser.2021.110732.
[35] W. Ai, L. Wang, X. Lin, S. Zhang, Y. Bai, and H. Chen, "Mathematical and thermo-economic analysis of thermal insulation for thermal energy storage applications," *Renewable Energy*, vol. 213, pp. 233–245, Sep. 2023, doi: 10.1016/j.renene.2023.06.009.
[36] N. R. Smith, J. Just, J. Johnson, and F. Karg-Bulnes, "Performance Characterization of a Small-Scale Pumped Thermal Energy Storage System," in *Volume 6: Education; Electric Power; Energy Storage; Fans and Blowers*, Boston, Massachusetts, USA: American Society of Mechanical Engineers, Jun. 2023, p. V006T09A012. doi: 10.1115/GT2023-104232.
[37] A. Albay, Z. Zhu, and M. Mercangöz, "State-of-Charge (SoC) Management of PTES Coupled Industrial Cogeneration Systems," in *Volume 8: Heat Transfer: Internal Air Systems; Heat Transfer: Internal Cooling; Industrial and Cogeneration*, London, United Kingdom: American Society of Mechanical Engineers, Jun. 2024, p. V008T16A005. doi: 10.1115/GT2024-128921.
[38] J. A. Dowling *et al.*, "Role of Long-Duration Energy Storage in Variable Renewable Electricity Systems," *Joule*, vol. 4, no. 9, pp. 1907–1928, Sep. 2020, doi: 10.1016/j.joule.2020.07.007.
[39] A. Amat Ventayol, J. S. L. Lam, X. Bai, and Z. S. Chen, "Comparative life cycle assessment of hydrogen internal combustion engine and fuel cells in shipping," *International Journal of Hydrogen Energy*, vol. 109, pp. 774–788, Mar. 2025, doi: 10.1016/j.ijhydene.2025.02.150.
[40] T. Lochner, R. M. Kluge, J. Fichtner, H. A. El-Sayed, B. Garlyyev, and A. S. Bandarenka, "Temperature Effects in Polymer Electrolyte Membrane Fuel Cells," *ChemElectroChem*, vol. 7, no. 17, pp. 3545–3568, Sep. 2020, doi: 10.1002/celc.202000588.
[41] C. A. Murphy, A. Schleifer, and K. Eurek, "A taxonomy of systems that combine utility-scale renewable energy and energy storage technologies," *Renewable and Sustainable Energy Reviews*, vol. 139, p. 110711, Apr. 2021, doi: 10.1016/j.rser.2021.110711.
[42] M. Hosseini, W. D. Lubitz, S. H. Tasnim, and S. Mahmud, "Optimization of hybrid renewable energy systems for remote communities in northern Canada," *Renewable Energy*, vol. 244, p. 122729, May 2025, doi: 10.1016/j.renene.2025.122729.
[43] Directorate-General for Energy, "The Vaskiluoto Heat Storage System: Vaasa's key project for an effective heat detox," *European Commission*. Accessed: Apr. 10, 2025. [Online]. Available: https://eu-mayors.ec.europa.eu/en/The-Vaskiluoto-Heat-Storage-System-Vaasa-key-project-for-an-effective-heat-detox
[44] L. Liu *et al.*, "Climate change impacts on planned supply–demand match in global wind and solar energy systems," *Nat Energy*, vol. 8, no. 8, pp. 870–880, Jul. 2023, doi: 10.1038/s41560-023-01304-w.
[45] M. Shirazi, "Realities of BESS in the Arctic," May 01, 2025.
[46] "Intensium® Max 20 High Energy," SAFT, May 2022. Accessed: Aug. 21, 2025. [Online]. Available: https://saft4u.saft.com/en/download_file/4136543b-59fc-4870-917e-a32248dd130a/English
[47] SAFT Batteries, "Saft energy storage system to help Svalbard decarbonize." [Online]. Available: https://saft.com/en/media-resources/press-releases/saft-energy-storage-system-help-svalbard-decarbonize
[48] S. Poux, "Homer Electric's energy storage system powered by Tesla," *Alaska Public Media*, Nov. 02, 2022. Accessed: Aug. 20, 2025. [Online]. Available: https://alaskapublic.org/news/2022-11-02/homer-electrics-energy-storage-system-powered-by-tesla
[49] M. Hobson, "On Kodiak Island, flywheels are in and diesel is 99.8% out," *Politico*, Jun. 10, 2016. Accessed: Apr. 10, 2025. [Online]. Available: https://www.eenews.net/articles/on-kodiak-island-flywheels-are-in-and-diesel-is-99-8-out/
[50] L. Pitorac, K. Vereide, and L. Lia, "Technical Review of Existing Norwegian Pumped Storage Plants," *Energies*, vol. 13, no. 18, p. 4918, Sep. 2020, doi: 10.3390/en13184918.

[51] J. Wang, H. Deng, and X. Qi, “Cost-based site and capacity optimization of multi-energy storage system in the regional integrated energy networks,” *Energy*, vol. 261, p. 125240, Dec. 2022, doi: 10.1016/j.energy.2022.125240.
[52] E. Benke, “How a sand battery could transform clean energy,” *BBC*, Nov. 04, 2022. Accessed: Apr. 10, 2025. [Online]. Available: https://www.bbc.com/future/article/20221102-how-a-sand-battery-could-transform-clean-energy
[53] “Vaasan Voima to grow the capacity of its thermal energy storage facility,” *Vassan Voima*, Oct. 12, 2024. Accessed: Apr. 10, 2025. [Online]. Available: https://www.vaasanvoima.fi/en/vaasan-voima-to-grow-the-capacity-of-its-thermal-energy-storage-facility/
[54] E. R. Zvereva, G. E. Marin, and I. G. Akhmetova, “Prospects for replacing traditional fuel for heat supply in the Murmansk region with hydrogen fuel,” *International Journal of Hydrogen Energy*, vol. 110, Feb. 2025.
[55] S. Kotian, A. Maliat, A. Azeez, and T. Iqbal, “Design and simulation of a hybrid energy system for Ramea Island, Newfoundland,” in *2022 IEEE 13th Annual Information Technology, Electronics and Mobile Communication Conference (IEMCON)*, Vancouver, BC, Canada: IEEE, Oct. 2022, pp. 0589–0595. doi: 10.1109/IEMCON56893.2022.9946552.
[56] “Arctic scientific research station in Yamalo-Nenets Region to begin work in 2025,” *TASS*, Jun. 21, 2022. Accessed: Aug. 20, 2025. [Online]. Available: https://tass.com/science/1469113
[57] V. Siberry, D. Wu, D. Wang, and X. Ma, “Energy Storage Valuation: A Review of Use Cases and Modeling Tools,” DOE/OE-0029, PNNL-32615, 1873889, Jun. 2022. doi: 10.2172/1873889.
[58] “HOMER Pro: Standalone Microgrids.” Accessed: Apr. 13, 2025. [Online]. Available: https://www.homerenergy.com/products/pro/index.html
[59] O. Schmidt and I. Staffell, *StorageNinja*. (2023). Imperial College London. Accessed: Aug. 22, 2025. [Online]. Available: www.energystorage.ninja
[60] RSMeans data, “Construction Cost Insights Report: Q4 2023,” *Gordian*. Accessed: Aug. 20, 2025. [Online]. Available: https://www.gordian.com/resources/q4-2023-construction-cost-insights-report/
[61] S. Cohen, V. Ramasamy, and D. Inman, “A Component-Level Bottom-Up Cost Model for Pumped Storage Hydropower,” NREL/TP-6A40-84875, 2004922, MainId:85648, Sep. 2023. doi: 10.2172/2004922.
[62] F. Nigbur, M. Robinius, and P. Wienert, “Levelised Cost of Hydrogen Calculator.” Accessed: Aug. 20, 2025. [Online]. Available: https://www.agora-industry.org/data-tools/levelised-cost-of-hydrogen-calculator
[63] S. Cohen and V. Ramasamy, “Pumped Storage Hydropower Cost Model.” Accessed: Aug. 20, 2025. [Online]. Available: https://www.nrel.gov/water/pumped-storage-hydropower-cost-model
[64] O. Schmidt, S. Melchior, A. Hawkes, and I. Staffell, “Projecting the Future Levelized Cost of Electricity Storage Technologies,” *Joule*, vol. 3, no. 1, pp. 81–100, Jan. 2019, doi: 10.1016/j.joule.2018.12.008.
[65] “Annual Technology Baseline: Utility Scale Battery Storage,” NREL. Accessed: Aug. 20, 2025. [Online]. Available: https://atb.nrel.gov/electricity/2024/utility-scale_battery_storage
[66] PNNL, “Energy Storage Cost and Performance Estimates.” Accessed: Aug. 20, 2025. [Online]. Available: https://www.pnnl.gov/projects/esgc-cost-performance/estimates
[67] *LCOH+*. Electric Hydrogen. Accessed: Aug. 21, 2025. [Online]. Available: https://eh2.app/lcoh/model
[68] SWECO Norge AS, “COST BASE FOR HYDROPOWER PLANTS,” *Norwegian Water Resources and Energy Directorate (NVE)*, vol. Veileder 3, pp. 96–99, 2012.
[69] S. Hanley, “China Developing World’s Largest Compressed Air Energy Storage System,” *CleanTechnica*, Dec. 27, 2024. Accessed: Aug. 21, 2025. [Online]. Available: https://cleantechnica.com/2024/12/26/china-developing-worlds-largest-compressed-air-energy-storage-system/
[70] Tesla Inc., “Select Megapack.” Accessed: Aug. 21, 2025. [Online]. Available: https://www.tesla.com/megapack/design

[71] "Storing Infinite Energy," Contemporary Amperex Technology Co., Limited. Accessed: Aug. 21, 2025. [Online]. Available: https://www.catl.com/en/uploads/1/file/public/202406/20240624152558_qft6x51t14.pdf
[72] W. Olis, D. Rosewater, T. Nguyen, and R. H. Byrne, "Impact of heating and cooling loads on battery energy storage system sizing in extreme cold climates," *Energy*, vol. 278, p. 127878, Sep. 2023, doi: 10.1016/j.energy.2023.127878.
[73] J. Jaewon and K. Panagiota, "A model predictive control strategy to optimize the performance of radiant floor heating and cooling systems in office buildings," *Applied Energy*, p. 68, Apr. 2019.
[74] Enersion, "Cost of Current Cooling Technologies." Accessed: Aug. 21, 2025. [Online]. Available: https://enersion.com/tips-tricks/cost-of-current-cooling-technologies/
[75] Y. Jiao, X. Dai, Y. Wang, L. Wei, H. Zhang, and H. Chen, "Case study on flywheel energy storage systems: LPTN-based transient thermal analysis," *Journal of Energy Storage*, vol. 120, p. 116319, Jun. 2025, doi: 10.1016/j.est.2025.116319.
[76] "Beacon Power Flywheel Energy Storage Systems," Beacon Power, Datasheet. Accessed: Aug. 21, 2025. [Online]. Available: https://beaconpower.com/wp-content/themes/beaconpower/inc/beacon_power_brochure_032514.pdf
[77] C. Murray, "World's largest 30MW flywheel energy storage project connects to grid in China," *Energy Storage News*, Sep. 19, 2024. Accessed: Aug. 21, 2025. [Online]. Available: https://www.energy-storage.news/worlds-largest-30mw-flywheel-energy-storage-project-connects-to-grid-in-china/
[78] "FINAL ENVIRONMENTAL ASSESSMENT FOR THE BEACON POWER CORPORATION FLYWHEEL FREQUENCY REGULATION PLANT, CHICAGO HEIGHTS, ILLINOIS (SITE 1), AND HAZLE TOWNSHIP, PENNSYLVANIA (SITE 2)," U.S. Department of Energy, Apr. 2011. Accessed: Aug. 21, 2025. [Online]. Available: https://www.energy.gov/sites/prod/files/2019/12/f69/final-ea-1753-beacon-power-2011-04.pdf
[79] A. J. Hutchinson and D. T. Gladwin, "Standalone and Hybridised Flywheels for Frequency Response Services: A Techno-Economic Feasibility Study," *Energies*, vol. 17, no. 11, p. 2577, May 2024, doi: 10.3390/en17112577.
[80] K. Mongird *et al.*, "Energy Storage Technology and Cost Characterization Report".
[81] S. Gebre, K. Alfredsen, L. Lia, M. Stickler, and E. Tesaker, "Review of Ice Effects on Hydropower Systems," *J. Cold Reg. Eng.*, vol. 27, no. 4, pp. 196–222, Dec. 2013, doi: 10.1061/(ASCE)CR.1943-5495.0000059.
[82] N. Walczak, Z. Walczak, and J. Nieć, "Assessment of the Resistance Value of Trash Racks at a Small Hydropower Plant Operating at Low Temperature," *Energies*, vol. 13, no. 7, p. 1775, Apr. 2020, doi: 10.3390/en13071775.
[83] S. W. Churchill and M. Bernstein, "A Correlating Equation for Forced Convection From Gases and Liquids to a Circular Cylinder in Crossflow," *Journal of Heat Transfer*, vol. 99, no. 2, pp. 300–306, May 1977, doi: 10.1115/1.3450685.
[84] "Domestic GSHPs," Ground Source Heat Pump Association. Accessed: Aug. 21, 2025. [Online]. Available: https://gshp.org.uk/gshps/domestic-ground-source-heat-pumps/
[85] J. Oerlemans and F. Keller, "Application of a simple model for ice growth to the Lake St. Moritz, Switzerland," *J. Glaciol.*, vol. 69, no. 276, pp. 1085–1090, Aug. 2023, doi: 10.1017/jog.2022.110.
[86] I. H. Bell, S. Quoilin, J. Wronski, and V. Lemort, "COOLPROP: AN OPEN-SOURCE REFERENCE-QUALITY THERMOPHYSICAL PROPERTY LIBRARY".
[87] Q. Liu, Y. Liu, H. Liu, Z. He, and X. Xue, "Comprehensive assessment and performance enhancement of compressed air energy storage: thermodynamic effect of ambient temperature," *Renewable Energy*, vol. 196, pp. 84–98, Aug. 2022, doi: 10.1016/j.renene.2022.06.145.
[88] F. J. Brooks, "GE Gas Turbine Performance Characteristics," *GE Power Systems*, Accessed: Aug. 22, 2025. [Online]. Available: https://www.gevernova.com/content/dam/gepower-new/global/en_US/downloads/gas-new-site/resources/reference/ger-3567h-ge-gas-turbine-performance-characteristics.pdf

[89] B. Bailie, “Compressed Air Energy Storage (CAES),” Siemens Energy, Aug. 2021. Accessed: Aug. 22, 2025. [Online]. Available: https://netl.doe.gov/sites/default/files/netl-file/21TMCES_Bailie.pdf
[90] Hydrostor Inc., “Goderich Energy Storage.” Accessed: Aug. 22, 2025. [Online]. Available: https://hydrostor.ca/projects/the-goderich-a-caes-facility/
[91] C. R. Matos, P. Pereira Da Silva, and J. F. Carneiro, “Economic assessment for compressed air energy storage business model alternatives,” *Applied Energy*, vol. 329, p. 120273, Jan. 2023, doi: 10.1016/j.apenergy.2022.120273.
[92] Institution of Mechanical Engineers, *Advanced Thermal Management in Future Hydrogen Fuel Cell Powered Vehicles*, (Jun. 08, 2021). Accessed: Aug. 22, 2025. [Online Video]. Available: https://www.youtube.com/watch?v=wol9w7qqKmI
[93] E. Van Der Roest, R. Bol, T. Fens, and A. Van Wijk, “Utilisation of waste heat from PEM electrolysers – Unlocking local optimisation,” *International Journal of Hydrogen Energy*, vol. 48, no. 72, pp. 27872–27891, Aug. 2023, doi: 10.1016/j.ijhydene.2023.03.374.
[94] M. D’Antoni, D. Romeli, and R. Fedrizzi, “Techno-Economic Analysis of Air-to-Water Heat Rejection Systems,” in *Proceedings of the EuroSun 2014 Conference*, Aix-les-Bains, France: International Solar Energy Society, 2015, pp. 1–8. doi: 10.18086/eurosun.2014.07.06.
[95] Battelle, “Manufacturing Cost Analysis of 1, 5, 10 and 25 kW Fuel Cell Systems for Primary Power and Combined Heat and Power Applications,” *U.S. Department of Energy*, Jan. 2017, Accessed: Aug. 20, 2025. [Online]. Available: https://www.energy.gov/sites/prod/files/2018/02/f49/fcto_battelle_mfg_cost_analysis_1%20_to_25kw_pp_chp_fc_systems_jan2017_0.pdf
[96] “Megawatt-Scale Fuel Cell Power Generation System.” Plug Power. Accessed: Aug. 22, 2025. [Online]. Available: https://resources.plugpower.com/gensure-stationary-power-fuel-cell/plug-megawatt-scale-fuel-cell-power-generation-brochure-north-america
[97] Electric Hydrogen, “EH2 Datasheet.” Accessed: Aug. 22, 2025. [Online]. Available: https://eh2.com/wp-content/uploads/2025/08/HYPRPlant-Spec-Sheet-Web-July-2025.pdf
[98] A. Badgett *et al.*, “Updated Manufactured Cost Analysis for Proton Exchange Membrane Water Electrolyzers,” NREL/TP--6A20-87625, 2311140, MainId:88400, Feb. 2024. doi: 10.2172/2311140.
[99] K. Mckeown, “Kyle Mckeown Electric H2 Interview,” Jul. 07, 2025.
[100] U. S. Meda, Y. V. Rajyaguru, and A. Pandey, “Generation of green hydrogen using self-sustained regenerative fuel cells: Opportunities and challenges,” *International Journal of Hydrogen Energy*, vol. 48, no. 73, pp. 28289–28314, Aug. 2023, doi: 10.1016/j.ijhydene.2023.03.430.
[101] ITM Power, “ITM Poseidon Datasheet.” Accessed: Aug. 22, 2025. [Online]. Available: https://itm-power-assets.s3.eu-west-2.amazonaws.com/POSEIDON_DATA_SHEET_2_7_2e1f89da3f.pdf
[102] Nel Hydrogen, “PSM Electrolyser Series.” Accessed: Aug. 22, 2025. [Online]. Available: https://nelhydrogen.com/product/psm-series-electrolyser/
[103] Z. Abdin, K. Khalilpour, and K. Catchpole, “Projecting the levelized cost of large scale hydrogen storage for stationary applications,” *Energy Conversion and Management*, vol. 270, p. 116241, Oct. 2022, doi: 10.1016/j.enconman.2022.116241.

The source code used to produce the results in this study can be found here:
https://github.com/msnowden729-alt/Arctic-Energy-Storage-Model